2018-01-01

Constitutive Model Development for Additive Manufacturing

Diana Berenice Montes
University of Texas at El Paso, d.berenice@hotmail.com

CONSTITUTIVE MODEL DEVELOPMENT FOR ADDITIVE MANUFACTURING

DIANA BERENICE MONTES CARRERA

Master's Program in Mechanical Engineering

APPROVED:

Jack Chessa, Ph. D, Chair

David Roberson, Ph.D.

David Espalin, Ph.D.

Angel Flores-Abad, Ph.D.

Charles Ambler, Ph.D.
Dean of the Graduate School

Dedication

Dedico esta tesis con mucho cariño a mis papás, Carlos Montes y Alicia Carrera a los cuales nunca dudaron de mi desde el principio de mis estudios. Que con su ayuda me ayudaron a trabajar cada día más y me mostraron el camino hacia el éxito.

Gracias a ellos quienes me acompañaron en mis noches de desvelo y aportaron todo el conocimiento en sus manos para poder avanzar y completar esta etapa en mi vida. Por todos sus consejos y palabras de aliento que siempre abundaron.

Hoy les agradezco y les digo que sin ustedes esto no hubiera sido posible.

A Dios, por haberme permitido tener tan maravillosos padres y miembros de la familia. A lo cual me bendice en cada paso que doy y en cada camino que tomo.

CONSTITUTIVE MODEL DEVELOPMENT FOR ADDITIVE MANUFACTURING

by

DIANA BERENICE MONTES CARRERA, BMSE

THESIS

Presented to the Faculty of the Graduate School of

The University of Texas at El Paso

in Partial Fulfillment

of the Requirements

for the Degree of

MASTER OF SCIENCE

Department of Mechanical Engineering

THE UNIVERSITY OF TEXAS AT EL PASO

December 2018

Acknowledgements

I would like to express special thanks to my thesis advisor Dr. Jack Chessa, Associate professor and Chair of the Mechanical Engineering Department. Dr. Chessa guided me and helped me to expand my knowledge throughout my master's degree. He dedicated his time to teach and help me complete this thesis with his willingness to support me to accomplish future goals.

To the mechanical engineering department, Dr. Lin and Dr. Love who always invest their time into teaching their classes with passion and by having interest in seeing their students succeed. They all have made a positive impact in my education throughout my bachelors' and master's degree.

I would like to thank my peers as well for supporting and encourage me to never give up. With their help, tasks became a learning experience and not only they were classmates but became friends.

Abstract

Additive manufacturing is known worldwide for revolutionizing the development of creating a three-dimensional piece by reducing the time and increasing its precision in each model. Over the last couple of decades, efforts have been made with the purpose of perfecting the additive manufacturing industry focusing on metals. One of the many divisions involved in this multibillion-dollar industry is Powder Bed Fusion. This category involves the use of thermal energy selectively fusing regions in a powder bed. As this technology has many advantages in the industry of 3D printing, there is still a lot of opportunity to perfect its results. The lowest number of defects has been the final objective to ongoing research for the creation of a functional 3D object. One of the main complications of this technology is the porosity involved in within the part and the residual stresses created. As a result, industry and academia perform aftertreatment processes to the parts in order to solve this consequential effect and optimize its mechanical properties. Often this tests and research have been completed by trial and error in which can waste resources. Another method utilized so that it is possible to reduce the overall efforts made, is the use of numerical models. These methods can simulate results with promising information in other to further investigate without losing valuable time and money invested in testing. For instance, Finite Element Analysis (FEA) is often used and recommended to easily change parameters such as: laser power, scan velocity and track distance. These results can be validated with simple related models with specific properties and boundary conditions.

Industry has ongoing research in a different area of additive manufacturing with material extrusion. As far as this category has been able to introduce itself in different aspects such as in aerospace, automotive and biomedical areas. In this category there are several advantages, for example having various industrial grade thermoplastics and it is relatively inexpensive there are

some disadvantages as well. For this paper some of the focus points selected are to explore material behavior in different ambient settings with validation examples though modeled geometries. Some of the research as well includes finite element analysis and examples of common behavior in creep and relaxation data.

Table of Contents

List of Tables

List of Figures

Chapter 1: Introduction

1.1 Thesis Outline

In the first chapter of the thesis is intentionally arranged to introduce additive manufacturing overall. Explaining the different categories and drawbacks seen over the years followed by introducing powder bed fusion. Material extrusion is also presented with theory and general information such as type and process in printing. As of chapter one, both technologies are introduced.

Chapter two focuses on powder bed fusion with subsequent categories that are integrated with sections mentioning published work, modeling, boundary conditions and testing of results. These sections 2.1 - 2.4 specify all Abaqus inputs mentioned with validation examples. These examples are shown with charts in 2.4 section detailing the results obtained. Chapter three includes second main category of material extrusion with description and published work. Subsequent categories of chapter three states model of exploration with PLA along with testing and conclusion.

Chapter four depicts the method seen throughout this work including the purpose in which they were made. Mentioning the meaning of the results stated and the explanation of each. Followed by chapter five that correlates with the previous chapter affirming the stage in which results are considered and what steps need to be made in the future. The appendix includes Abaqus inputs that contain all boundary conditions and material properties previously mention set for the test to run.

1.2 Background

The recent popular term as 3D-printing is one of the most growing industries in the world. There are numerous terminologies that refer to this method and are utilized as a denomination of such technology. Some of the used names are: rapid prototyping, 3D printing or additive manufacturing. Its technical term is additive manufacturing in which consist of a set of diverse categories that can be utilized in many professions around the world. The process of additive manufacturing pertains of laying out material upon layer by layer utilizing a computer-based model or prototype.

In contrary to the traditional metal processing approaches such as subtractive manufacturing or tooling. These formative popular methods include shaping, casting, forging, and machining to name a few. Additive manufacturing surpasses and presents an enormous advantage as to manufacture a precise model that will require the minimum amount of material with the inclusion of supports. In comparison with both methods, in subtractive manufacturing a higher amount of material is wasted and disposed in order to produce a model of the desired output. With additive manufacturing the industry will be able to produce complex, lightweight and existing assemblies of materials without any tooling and minimum amounts of post-processing. Different materials commercially available can vary from ceramics, composites, metals and more. Many research laboratories are determined to expand the amount of materials so there is no underlying limit and increase the capability of this technology.

Industry and universities invest in training students for the benefit of increasing knowledge and expanding skills. Classes are provided, and laboratories dedicate themselves into participating in industry projects. The first step into producing an existing model is by designing a CAD (computer aided design). Converting the file into. STL for the slicing software. Followed by

slicing and layering with a tool path for the printer for the three-dimensional object as the final result (Post processing may be needed of the manufactured part). As of 2012 the American Society for Testing Materials (ASTM) published ASTM F2792-12a standard in order to determine and sort the difference in the categories of processes and methods for additive manufacturing. A total of seven categories exist and within the model tree each has different capabilities with its designated equipment.

1.2.1 Additive Manufacturing

Main categories in additive manufacturing include:

1. Vat Photopolymerization
2. Powder Bed fusion
3. Binder Jetting
4. Material Jetting
5. Material Extrusion
6. Sheet Lamination
7. Direct Energy Deposition

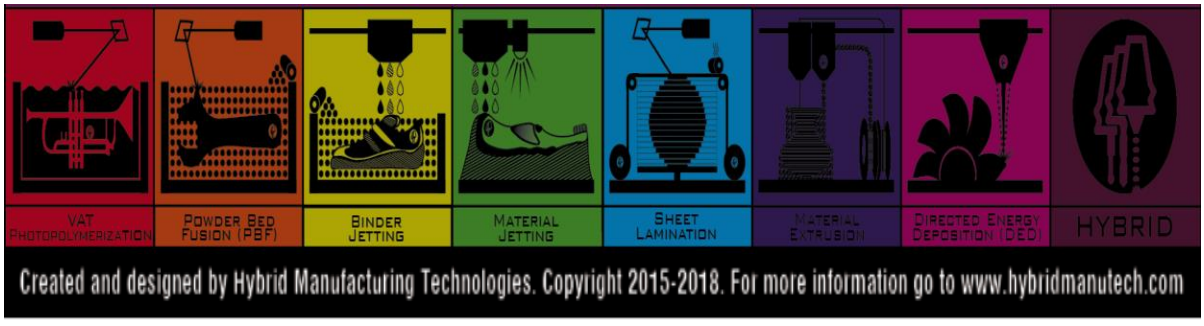

Figure1: Additive Manufacturing Categories [1]

Chapter 2: Additive Manufacturing: Material Extrusion

As mentioned before in the categories involving additive manufacturing material extrusion is one of the most commonly used branches in the three-dimensional printing industry. There are a variety of products starting from a couple of hundred dollars in value to thousand-dollar worth machines. Mostly used for educational purposes and openly introduced to schools and universities to extend research of this matter. Currently the University of Texas at E Paso owns a 3D printing lab (Design Studio) open for students in order to complete class projects and research. Owning more than 8 MakerBot machines, 2 Cube printers, and 1 U-print. As well as mentioned before there is an alternate private lab in The Keck Center that does only research with material extrusion as well. Both are for research purposes with the only noting difference that the Design Studio lab is open for student including walk-in hours used for any related class or for research. These are only of engineering students since the purpose of the lab is to facilitate students with working projects and for them to get introduce and engage in 3-D printing. For this research the equipment used consists of the Micro M3D printer.

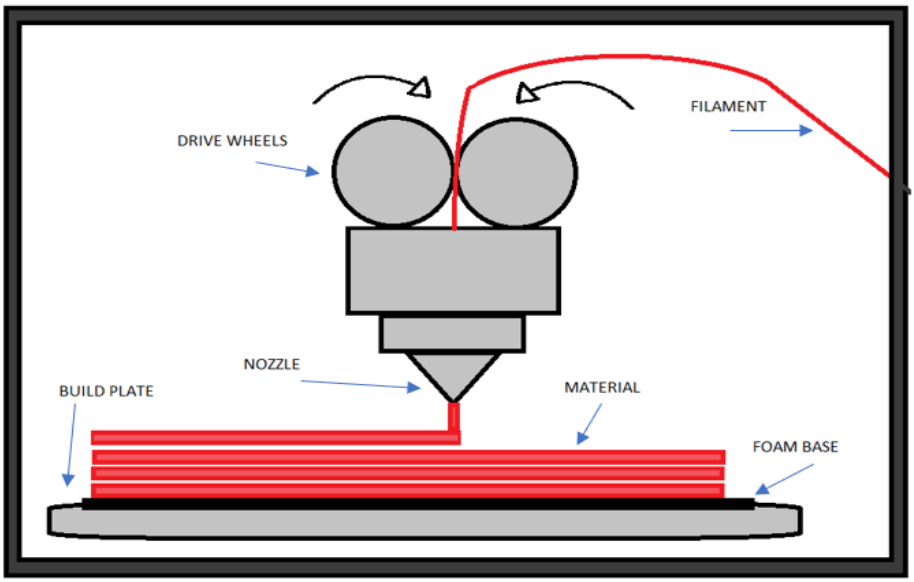

Figure 2: Simple Schematic of Material Extrusion

Material extrusion consists of a simple layout using gears that feed the filament used through a nozzle once it reaches a specific temperature for a constant flow. As one of the most common categories a correct term for this process is Fuse Deposition Modeling (FDM). This category was developed by S. Scott Crump in 1988 and not until 1990 it was commercialized by Stratasys Inc. This only contains plastic filament extrusion (thermoplastic pellets). This filament is available in different colors with constant diameters and no thermal degradation.

Material extrusion process consists of loading the filament (material) into the machine, in which they most commonly have a preset function or button. This will heat the nozzle in order to make the loading process easier without any damage to the material itself. This is also known as "Liquefaction" meaning it slightly melts the material enough to load the machine. At this point the extrusion part of the process begins, with the gears pulling the filament until material is out the nozzle. Since it's a simple procedure with mostly utilizing gears, filament and heat to lay the material upon a heated bed to complete the geometry desired until solidified.

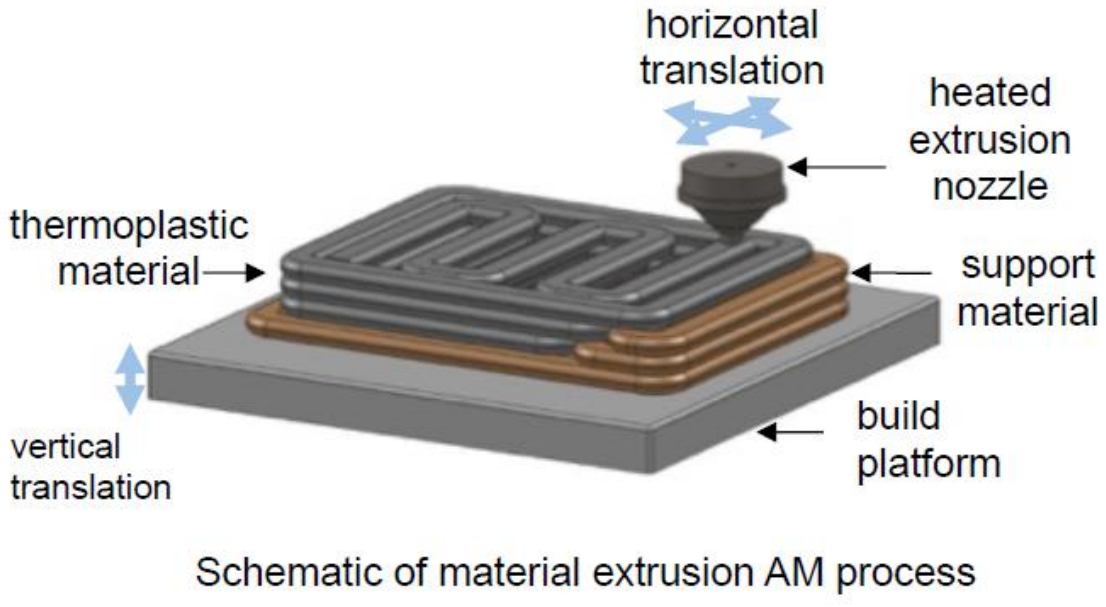

Figure 3: The W.M. Keck Center Schematic of material extrusion [2]

2.1 Advantages and Materials

The advantages of utilizing this method are that industrial grade of thermoplastics can be used, inexpensive, water soluble support materials. Even though material extrusion is very useful the material is limited since most of the machines use only either PLA or ABS. The resolution can be limited to a certain level due to the extrusion tip. Parameters are often modified in order to obtain a better result, such as changing the orientation of the part depending on the geometry desired and support assigned. Another issue often seen is that sometimes when the bed (platform) is unbalanced or either the nozzle or bed are not heated properly the interlaying bond is not 100% fused together.

Table 1: Material Extrusion: Material industrially available

Material	Notes
ABS 30	Stable UV
PLA	High strength, high stiffness
Polycarbonate (PC)	Strong tensile properties, medium range temperature tolerance
PC-ABS	Strong for power-tool prototyping
Nylon 12	High fatigue resistant, tough
ABS-ESD7	Requires static dissipation
ABSi	Used in translucent components

Material	Max. Extrusion Temp	Max. Oven Temp.
ABS-M30/M30I	320 C	95 C
PC-ABS	330 C	110 C
PC/PC-ISO	365 C	145 C
PPSF	415 C	225 C

Figure 4: Material Specifications [3]

Material is available and can be modified from the start of defining the contours, printing axis, support material and the fill-in space of the material being printed. Several parameters are involved as well as coding. For the purpose of this work only material extrusion with a Micro M3D printer is used. As well as modeling creep and relaxation information for published work and as well as performing a simple validation test of viscoelastic material with creep and relaxation data.

2.2 Methodologies in Research

Viscoelastic material is known as a material that shows a behavior with viscosity and elasticity that can resist a shear flow in relationship with time when stress is applied. It as well has a geometrically linear behavior, this occurs and several different relaxation times. There are two types of responses of material that can be investigated through two different testing methods. For the first categorized behavior can occur within less than one second. Meaning that the material behavior response has a short or small relaxation time. For this some dynamic testing can be performed including frequency. Setting a constant frequency range and an oscillating incentive.

With a larger response (1 second to an hour) another time of behavioral testing can be implemented, this experiment is called the creep and relaxation testing. Creep is when a load is applied and is left constant creating deformation. On the other hand, Relaxation occurs when a material is under constant stain. Both of these are time dependent and contribute on deformation on the material, permanent and recoverable.

Whenever these tests are performed, they often involve a set of equations and types of systems that could help understand its behavior. As mentioned in this work, creep and relaxation are to explore the behavior on PLA by analyzing creep and relaxation tests.

2.3 Creep and Relaxation

As previously mentioned, when a material is submitted to a constant stress and is time-dependent it undergoes to a process divided in three stages, primary creep, secondary creep and tertiary creep (I,II III) [4]. This process can be obtained when material undergoes or is submitted to high temperatures (As well as room temperature but is often rare and in only certain materials). When a constant load (tensile stress) and a high temperature the material tends to deform. The deformation or stress applied can occur when it is lower than the yield stress of the material. Material's original length now increases until it reaches its breaking point. Presented below in Figure 5, creep curve is shown with the different stages separated.

In the first stage called the "Primary Stage" we can denote that average strain is rather high and as time increases strain proceeds to decline. In Secondary Stage in present strain reaches a rather or just about constant rate. As for the last stage "Tertiary Stage" necking now is present in the material and strain rapidly increases at an exponential rate. At this stage fracture commonly occurs, due to the material reaching its ultimate stress limit point.

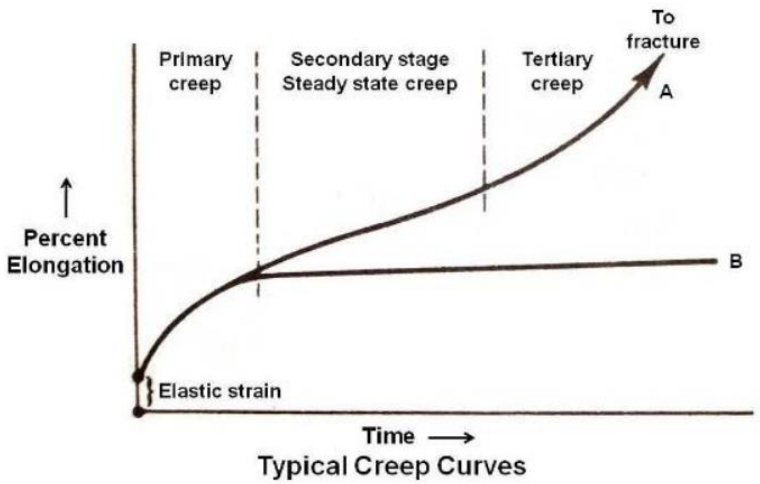

Figure 5: Graph of three stages of creep [4]

Even though this creep and relaxation tests are commonly used for metal materials and researching into dog-bone specimens. It can as well be applied for different materials, stating the expected results and limits for each material beforehand. As far as the analyzing PLA for this paper it can be said that the objective is to replicate as much for future testing with the standard model of a dog-bone geometry.

Not only it is mentioned in publications that creep and relaxation testing have been performed but in order to proceed with that stage in the process it is often analyzed by a mathematical approach. This leads into researching and solving some presented models that are often represented in these cases. As well there are different types of testing into looking for time dependency in a material constant stress resistance, there are as well three main mathematical models that will be analyzed.

Looking into creep behavior, four models are analyzed, Maxwell model, Voight model, Kelvin-Voight model, and Burgers model.

Maxwell model: A model in which is the most basic and general model that focuses on a linear model with viscoelasticity. Its configuration is assembled in a parallel manner.

$$F=K_eX_e = K_v(\frac{dX_v}{dt}) \quad \text{Eqn. (1)}$$

Where Ke is the spring constant (ratio of force and displacement)(N/m), and Xe is the spring's displacement. In this case the formula yields to Kv, that signifies the ratio of velocity and force with units of Ns/m. Kv is as well multiplied by the derivation of Xv with respect to time. Xv is the displacement of the dashpot[8].

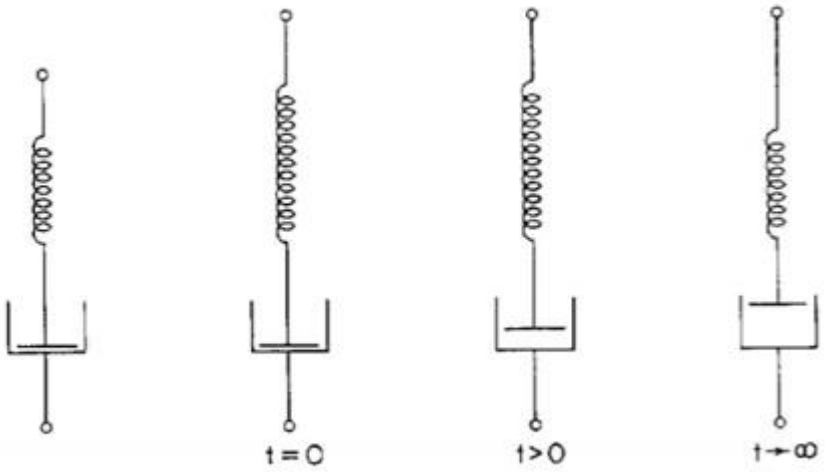

Figure 6: Stress Relaxation model [5]

2.4 Modeling

Research has also been a big part of using final element analysis in such a way that resources are continuously been drained in testing. Time and money are an important factor that helps that outcomes can be accomplished. The intended purpose of this research is to utilize a method that can save efforts and still predict and obtain congruent results in a fast timeline. For this utilizing Abaqus to obtain output data of PLA behavior, in which two states of a material are

being considered. These two consists in analyzing PLA material through a nozzle that is considered in the solid phase. As well as the main direction of the research of considering the materials properties when material becomes viscoelastic obtaining creep and relaxation information. Two of this method are being investigated through Abaqus property inputs and boundary conditions.

A sample was submitted to a desktop 3D printing machine in which a piece of PLA was introduced to obtain the distance displacement as it was being videotaped and measured. This material was measured into 1 in. (24.5 mm), the distance was recorded to be a total of 1.2 in (31.85 mm) after 63 seconds. This was considered to be a set of value inputs that could later be added into the boundary conditions of Abaqus so there can be creeping values as well as relaxation. Since this is an exploration research of the material, some of this point were calculated through interpolation since they are a rough or approximation of the value that can be detected in the test and video. As well as it is a simple test the values are subject to change depending on the test being perform and a change of desktop printers can make the information vary. For this test they are only utilized for the whole purpose of imputing possible values of creeping in PLA.

Continuing with the testing as mentioned a total of 1 in in length of PLA was utilized. For the modeling parameters it was decided to model a total of 30 mm of PLA in length and a width of 1mm. A nozzle was as well simulated and modeled with a similar shape of an original nozzle.

Nozzle was modeled with a total width of 2.5 mm, these includes different width measurements since the original shape is not symmetrical and a total length of 35 mm. These models were created with the simplest possible geometry that will make the FEA focus only on the filament's reactions and behavior when all conditions are set. These geometries are shown in the following

images below with the Abaqus model. Filament is purposely set in the nozzle to simulate the correct process of fused deposition melting. In this case filament is set in Abaqus with a contact condition. Both models are shown, modeled and tested with x-symmetry.

Table 2: Nozzle modeled dimensions

Nozzle	Dimension (mm)
Total width	2.5
Width 1	1
Width 2	1
Length	35

Table 3: Filament modeled dimensions

Filament	Dimension (mm)
Length	30
Width	1

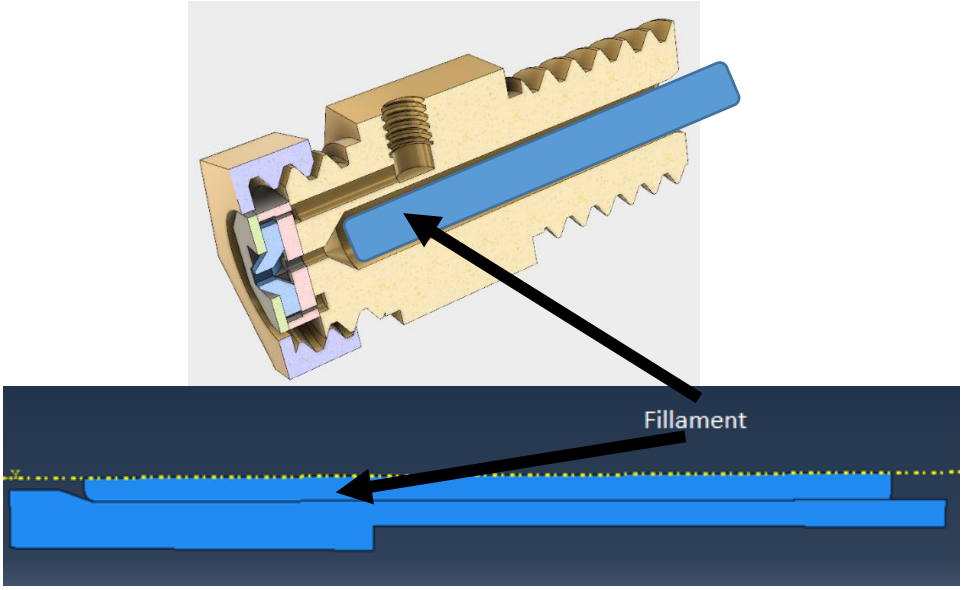

Figure 7: Modeled Nozzle and Filament [6]

2.5 Boundary Conditions

For Abaqus input properties both filament (PLA) material properties and Steel (nozzle) are being considered. Yield and plastic stress and strain were calculated respectively. These properties include conductivity, mass density, young's modulus, poisons ratio, and specific heat for both materials.

Boundary conditions were considered as well as part of the assembly to verify that test being performed matched the research done through testing with the 3-D printer as well in Abaqus. As mentioned, two separate parts were created (filament & nozzle) and submitted as an assembly. A section was created for both of the parts. Type entered was a solid, homogeneous with a plane stress/strain thickness of 1. An instance was set for both of the sections with a Datum (csys-1) as an added feature. Since the assembly contained two different parts a contact condition was set in between the two surfaces of the parts. Initial steps are automatically added by the Abaqus software, in addition to that an adiabatic extrude step was selected. For this step it was set as a coupled temperature-displacement type with a transient response. A total of 10 seconds were included for the time period and an automatic stabilization to specify the damping factor of

0.0002. The stabilization ratio to strain energy was as well selected as 0.05 as the maximum value. In the incrementation of this step it is set as automatic with a maximum number of increments of 10,000. The initial increment size was determined to be for initial of .001, a minimum of 1E-6 and a maximum of 0.01. A maximum allowable temperature change per increment of 50. The equation solver of matrix storage is selected to use “Use Solver Default” with a solution technique as “Separated”. Lastly the default load variation with time was set to be instantaneous with a linear extrapolation of previous state at start with each increment.

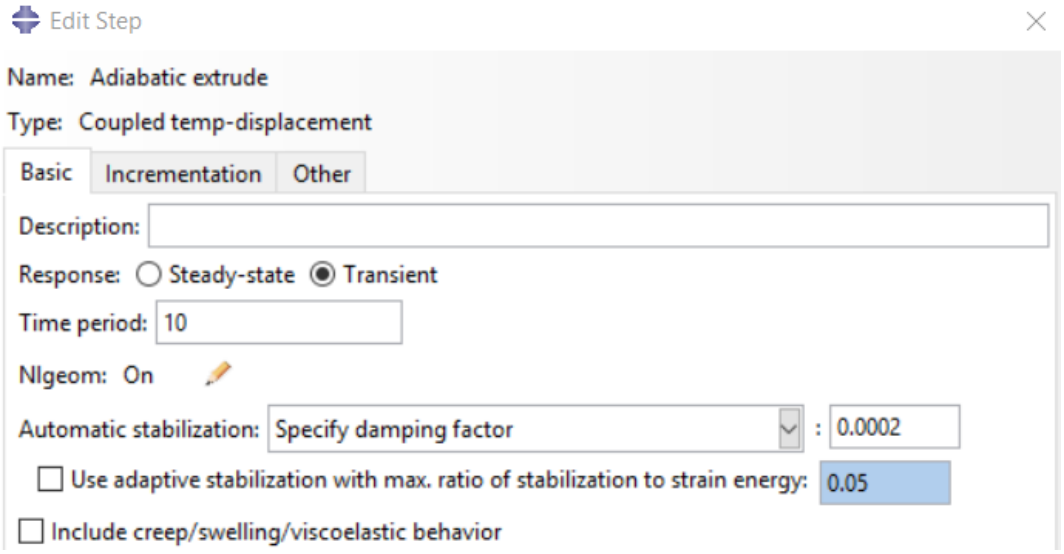

Figure 8: Basic selection in adiabatic extrude step

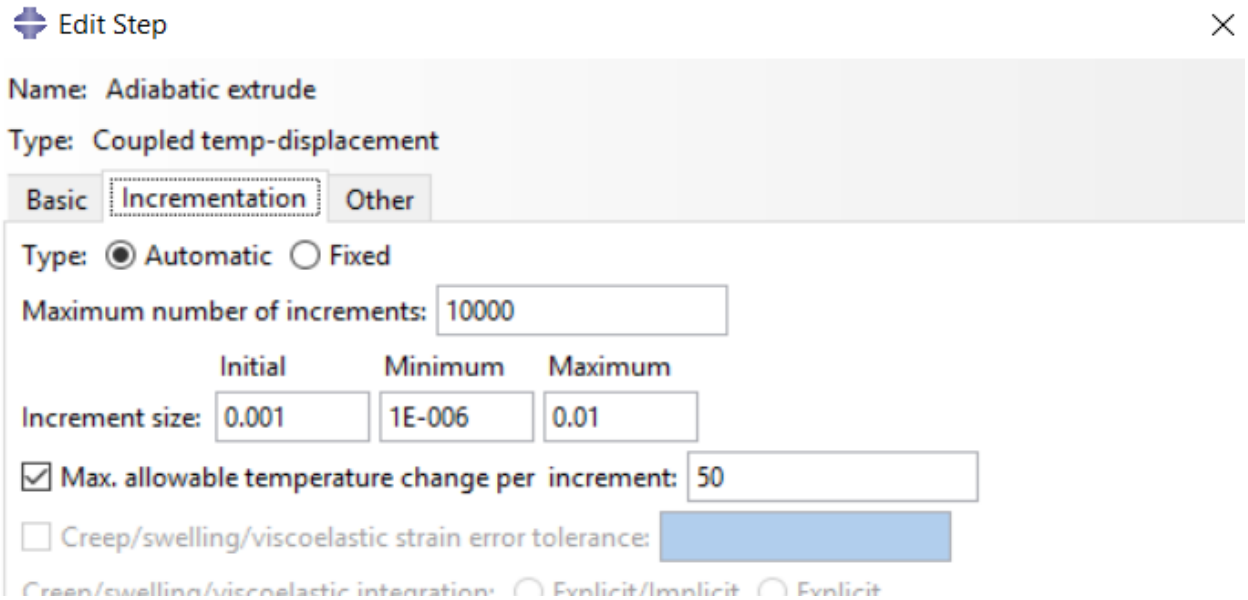

Figure 9: Incrementation selection in adiabatic extrude step

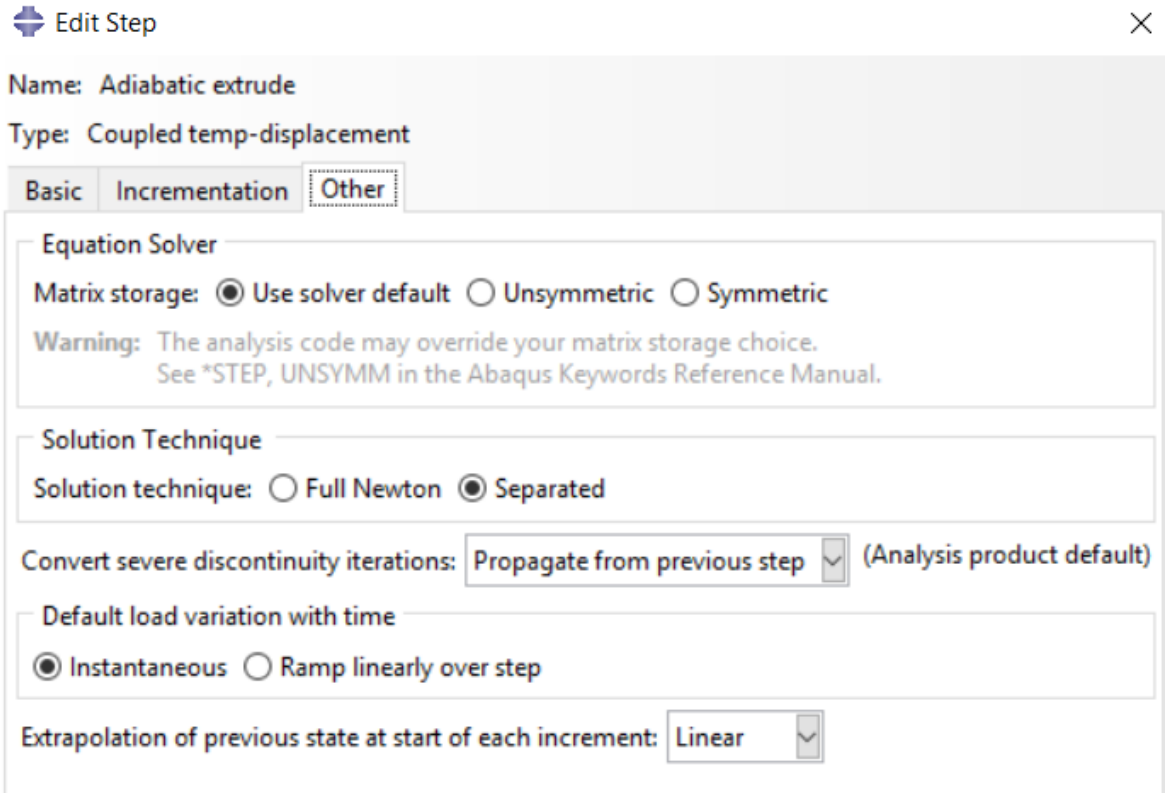

Figure 10: “Other” selection in Step

As previously stated, a contact interaction was set between the two models. This included a tangential behavior selected with a friction coefficient of 0.2 and isotropic directionality selection. As well as a normal behavior with a pressure-overclosure set as “Hard” contact. The constraint enforcement method set as “Default” with the option of separation after contact section selected. Another condition utilized is an amplitude with a time span of “Step time” that uses default solver. A tabular selection of time and frequency with amplitude dependency. Starting both sections with zero up to and amplitude of 1 and a time/frequency of 2.

An important part of the test is the way the main boundary conditions are selected since it simulates the material accordingly. If there is a change or a miscalculation of the data results can vary and not validate the results. For this test the load selected includes heat flux and an extrude

pressure. For the adiabatic extrude step (coupled temp-displacement) mentioned the load selected is attached contemplating both inputs. A surface heat flux was selected as the type with the region manually picked and showed by the arrows shown in figure 12below which will demonstrate direction and surface placed. A uniform distribution of f(x), a magnitude of 1 and an instantaneous amplitude. Another load was added as mentioned, including an extruded pressure similarly connected to the step. A uniform distribution considered with a total magnitude of 0.07 and an amplitude ramp of 2 seconds. A nozzle fixation is included as well with a type of displacement/rotation connected to the adiabatic step. A uniform distribution only selectin U2 as the base of the axis being analyzed and an instantaneous amplitude.

Lastly a predefined field selection with a temperature type for the initial step with a picked region. A direct specification distribution f(x) designated and a section variation that will be constant through the region with a magnitude of 100.

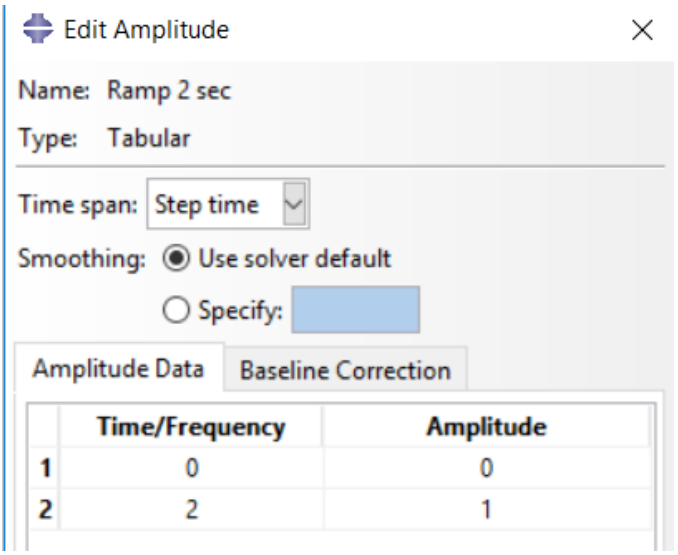

Figure 11: Tabular amplitude in Abaqus

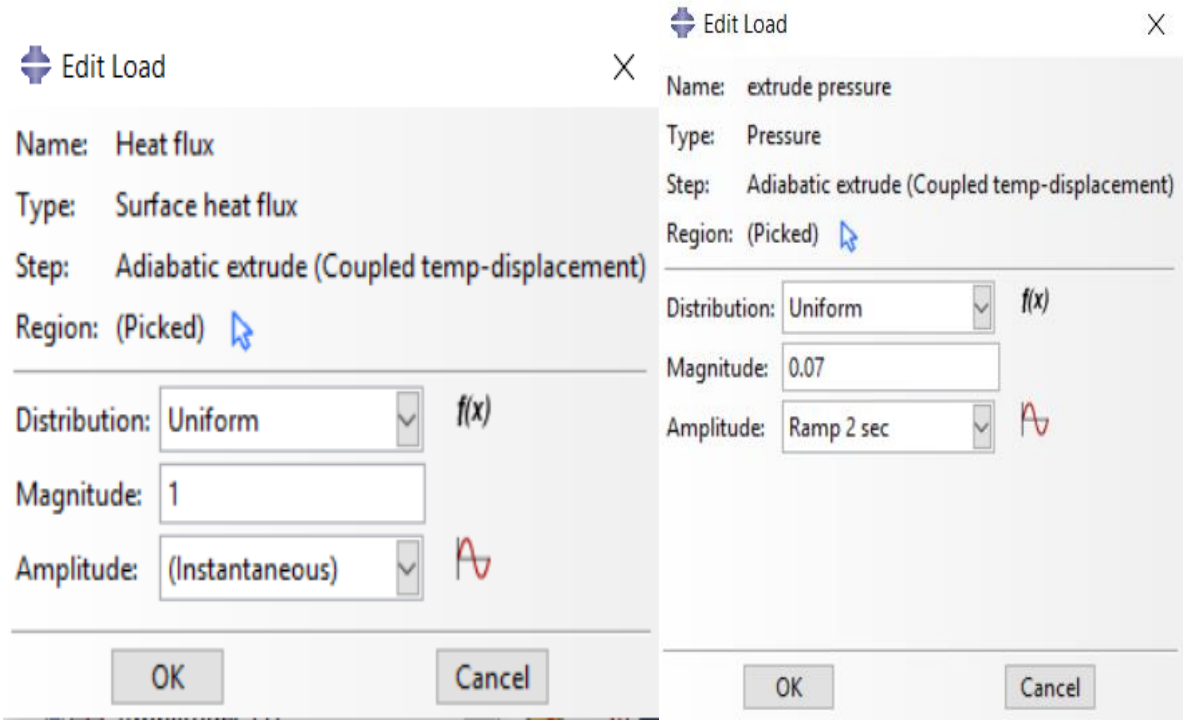

Figure 12: Heat flux and Pressure Loads

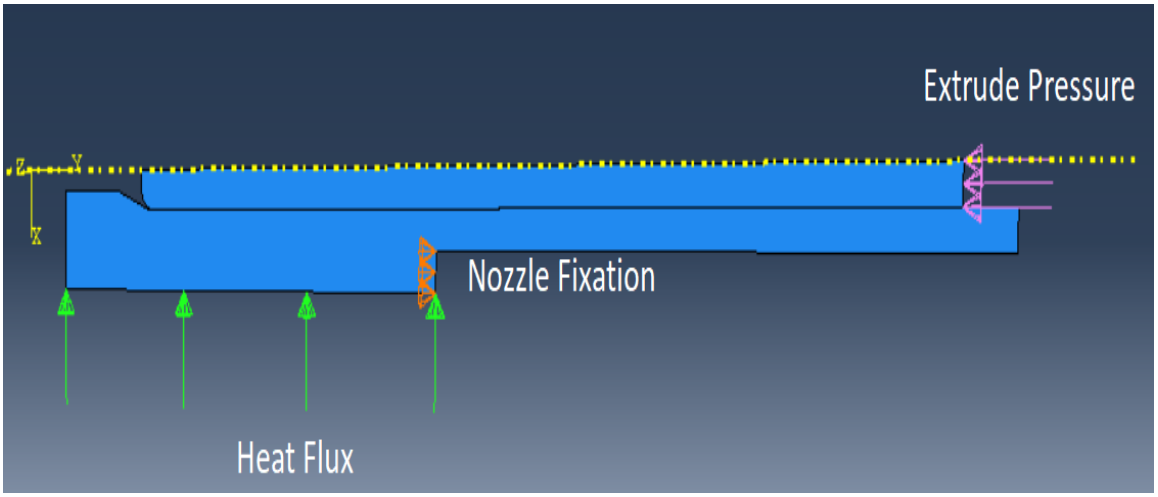

Figure 13: Boundary conditions & Load direction

2.6 Meshing

Meshing is an important aspect when considering precise results. In this case a specific meshing type was selected due to the complex geometry of the model. Behavior analysis in this test is carefully observed and recorded due to the goal of this research of exploring the material. Mesh selected is called Arbitrary Lagrangian-Eulerian (ALE), or adaptive meshing according to Abaqus [7]. This type of meshing allows the domain to follow the material throughout deformation without distorting the original shape or structure of the mesh. For the Lagrangian part of the meshing it causes the nodes selected to move a flow in connection to the points created for the material, however in the Eulerian part nodes are fixed and material flows in within the mesh. Connecting both motions is constrained only in parts required at deformation.

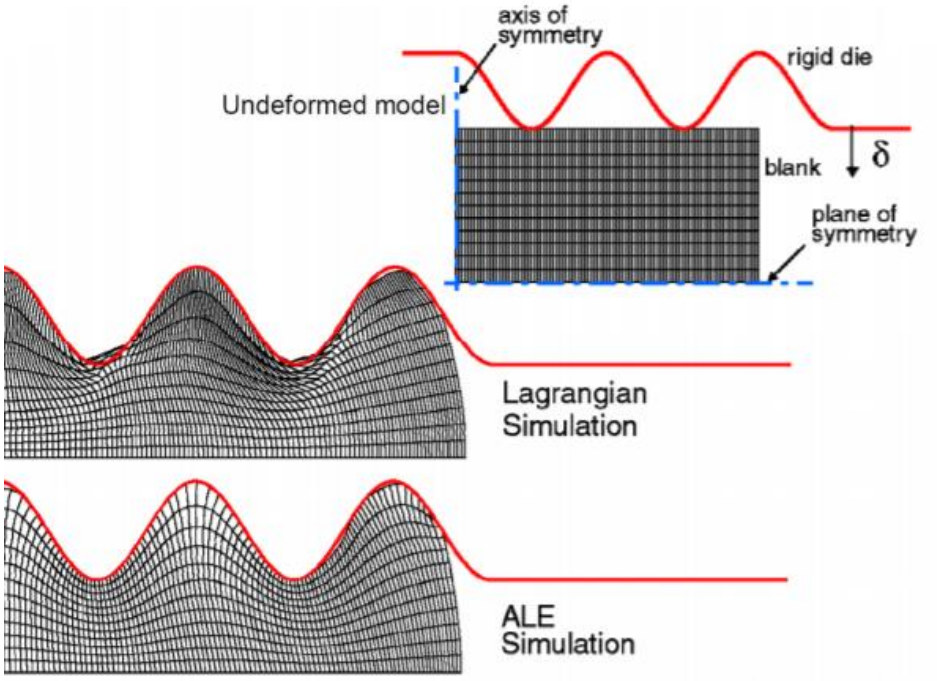

Figure 14: Arbitrary Lagrangian-Eularian meshing [7]

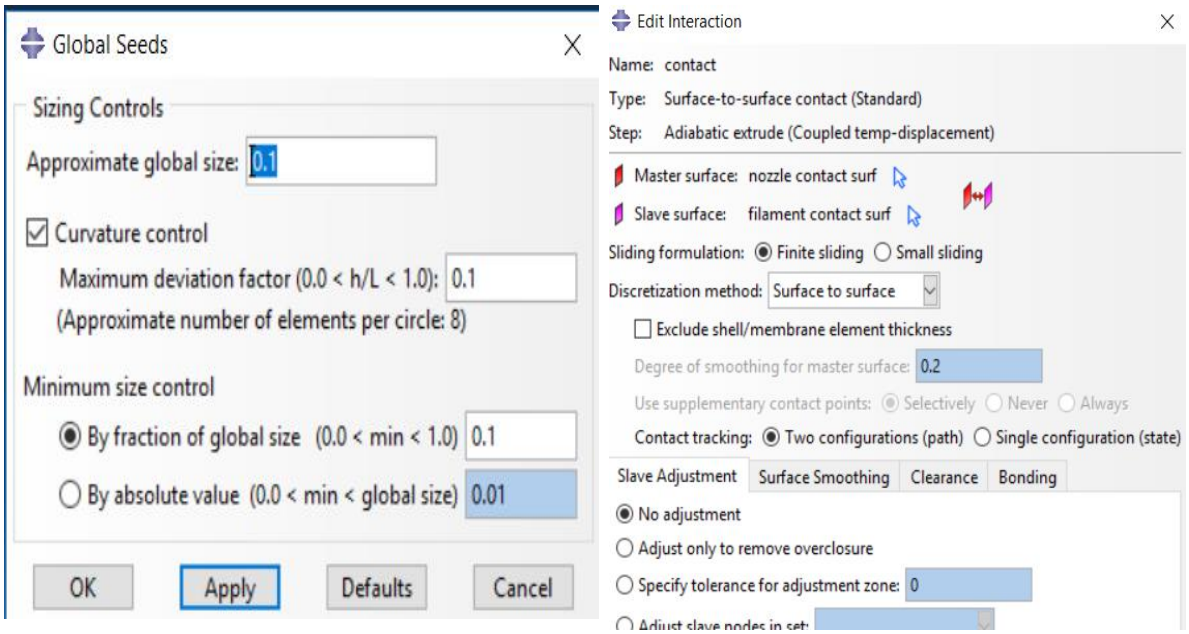

Figure 15: Meshing and Interaction input in Abaqus

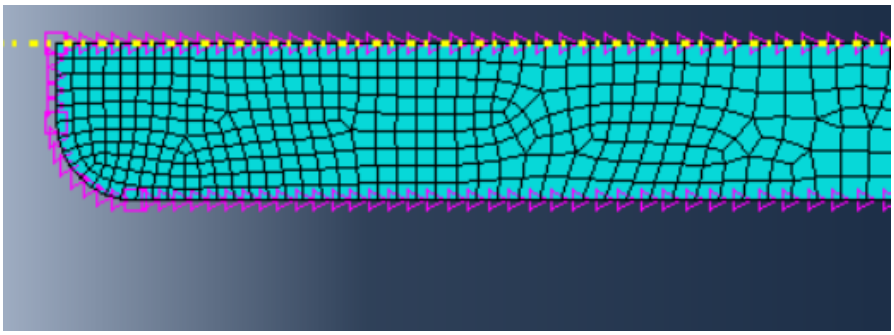

Figure 16: Meshing with selected seed edges

2.7 Analysis and Equations

For the first part of the testing the material was considered as solid and without a considered flow. For the second part of the conditions a viscoelastic material was designated including the area, stress and strain. An Abaqus selection of creeping material information can be determined by three methods, shear, volumetric and a combined test data. Setting the domain to be considered by time and selecting a volumetric data information can be obtained with the long-

term normalized volumetric compliance or modulus. As well as for the tabular section for the bulk compliance (jK) or relaxation test data(kR) and time in seconds. Stating the main equations used as follows.

Area of a cylinder to simulate filament geometry since diameter is available and length chosen randomly.

Area of a cylinder $A = 2\pi rh + 2\pi r^2$ Equation. (2)

Stress and strain are also calculated for this reason as volumetric compliance was chosen in Abaqus. For volumetric compliance it was necessary to calculate the effective load being applied and the normalized stress. Considering the previous stated length of Lo as the original length by 1in (24.5 mm) and the final length of 13 in (31.85).

Stress $\sigma = \frac{(L-y)\rho}{A}$ Equation (3)

Strain $\in = \frac{(L-y)\rho}{AE}$ Equation (4)

Effective Load $P_{eff} = \frac{\rho L}{2}$ Equation (5)

The volumetric compliance a bulk modulus equation determine the compressing of a material when submitted to pressure. This ratio in volume includes the fractional volume with the units of Newtons per meter squared.

Bulk Modulus $B = \frac{\Delta P}{\Delta V/V}$ Equation (6)

For this, original equations they are only considered for Abaqus while in the theoretical consideration of this is though the Maxwell model mentioned [7]. The image below is a visual representation of the models that can be considered when solving viscoelasticity problems. A creep and relaxation graph are also shown for each of the possible models.

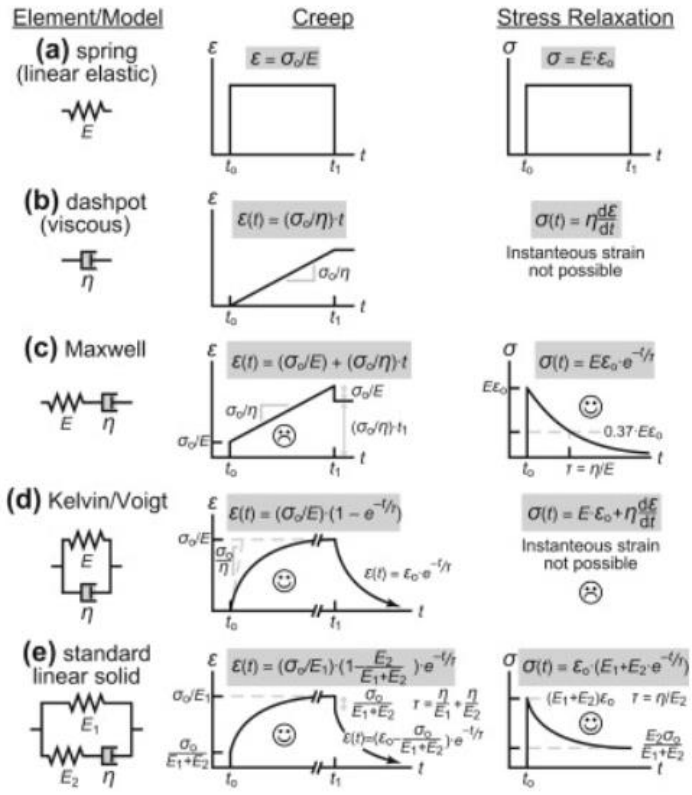

Figure 17: Element models with creep and relaxation graphs [8]

2.8 Testing and Results

A total of two tests were performed in this research focusing on solid material with filament and nozzle properties and viscoelasticity. The first test mentioned was done to acknowledge properties and researching filament behavior after some simple boundary conditions set. Stress recoded in figure below can be denoted as minimal, however downward

flow is considered insufficient. A set of sub sequential test are necessary in order to validate information to use in additive manufacturing in the future. For the second test information extracted from the experimental and recorded procedure by the Micro M3D printer. This test consisted of selecting a definite amount of filament and let it run through the nozzle. Later the displacement of the filament was measured and recorded with respect to time. Original length was recorded to be 1 in (24.5 mm) and the final length of 1.3 in (31.85 mm). Time in seconds recorded to reach the final length was of 63. Data was interpolated in between the initial and final point in order to obtain a varying amount of points. This data was interpolated with a 15 second interval after the second point.

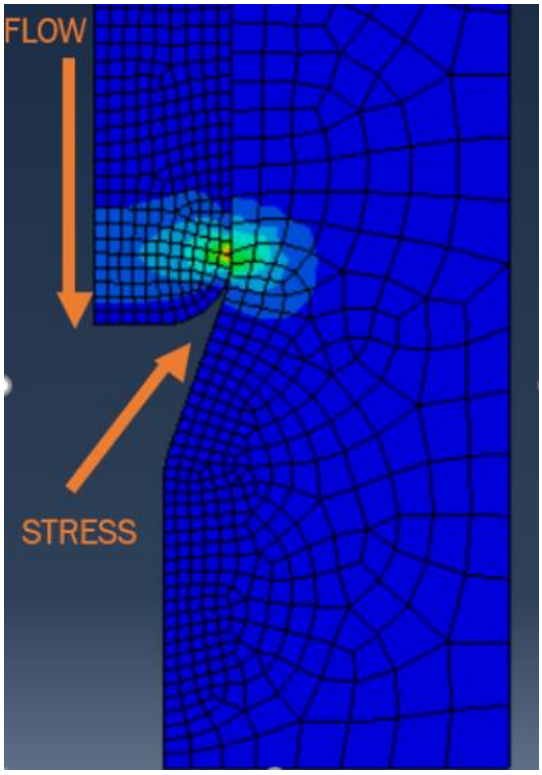

Figure 18: Resulting stress with minimal flow

Chapter 3: Powder Bed Fusion

As previously mentioned, the branch of powder bed fusion is relatively new and two of their main subsections are Electron Beam Melting and Selective Laser Melting. There are various commercially available equipment systems that will be displayed in the following chart.

Process	Equipment	Build volume (mm)	Energy Source (W)	Type
EBM	ARCAM	200x200x350	700	Electron beam
LM	Concept Laser	300x350x300	200	Fiber Laser
LM	MTT	250x250x300	100-400	Fiber Laser
SLM	Phenix System	250x250x300	500	Fiber Laser
SLM	Renishaw	245x245x360	200 or 400	Laser
SLM	Realizer	250x250x220	100,200,400	Laser
SLM	Matsuura	250x250 (Ø)	400	Fiber Laser/Hybrid
DMLS	EOS	250x250x325	200-400	Yb-Fiber Laser

Figure 19: Additive manufacturing systems, process and energy source

In the list shown above details are introduced for each machine, a set of four are located at The University of Texas at el Paso. The research laboratory “The Keck Center” takes the advantage of completing full investigations, as well as modifying its parameters and continues upon testing for the revolutionization of additive manufacturing with metal powders. As part of the same family of metal printing production, the materials offered are numerous. For the purpose of researching the material lacking academic investigations of Aluminum, selective laser melting will be furthermore studied.

As of 2006 SLM Solutions was the first company in the development of a process for mainly Aluminum and Titanium powders. This German metal manufacturing pioneer company also associates with industrial group Siemens for the production of gas turbines and blades. One of their biggest advantages are, that they are able to reduce lead time and finish their products up to eleven times faster that with traditional machining. To increase their popularity, NASA utilized this method into a rocket engine injector as it was depicted in a press release. As part of their highlighted assets, NASA recognized a key feature of SLM Solutions. They stated the benefit of SLM allowing assemblies directly form printing as a whole finalized assembly. Reducing the process of printing separate individual parts followed by completing the assembly. This machine contains of a laser source with scanning mirrors that reflect into a lens directly sourced to a thin layer of powdered metal. For this, the layer is applied in the build platform by a powder scraper (recoating mechanism/leveling instrument). After laser selectively fuses powder together a melted metal pool is then lowered. Continuing with the next layer set, this step is repeated in order to complete a full prototype layer upon layer. Below is presented an image depicting an equipment representation of an SLM detailed schematic.

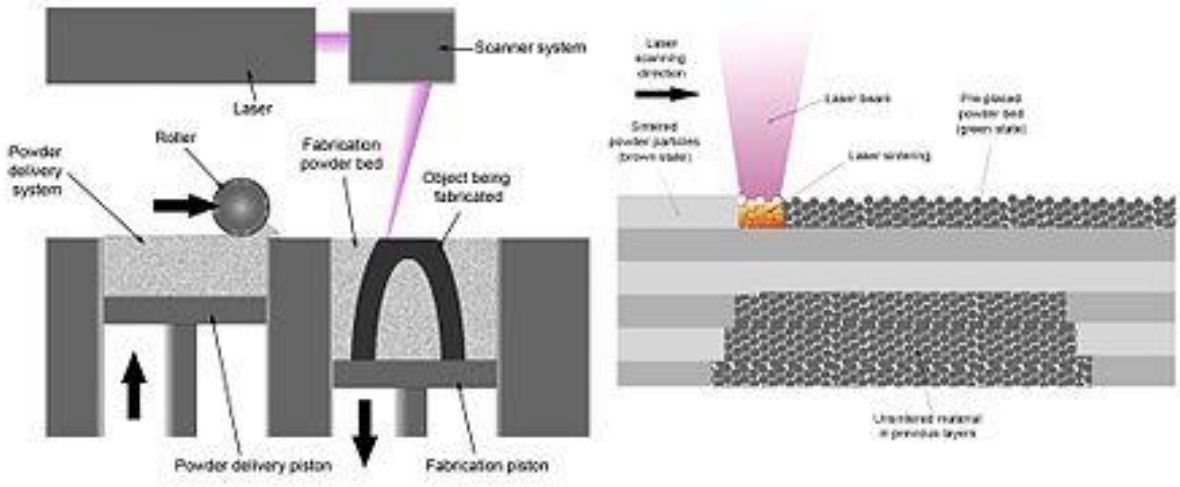

Figure 20**:** Selective Laser Melting schematic [9]

3.1 Additive Manufacturing: Metals

The importance of metals is such that they are able to plastically deform in considerable amounts without compromising its uniformity. As well as the high melting point that consists of an average of 1000 C. Additive Manufacturing has been present in the last couple of decades, but it can be argued that not until recent times that the fabrication of metal prototypes has been introduced to the industry. As far as printing metals additive manufacturing could not compete with the traditional manufacturing until now, for instance forging, casting and powder metallurgy (PM). Since then it is a method that has been emerging and it is now as important in the industry as other composites, ceramics. For this a series of applications have been implemented and utilized. As of March 2016, the American National Standards Institute (ANSI) and America Makes published the "America Makes & ANSI Additive Manufacturing Standardization Collaborative" which sightsaw the surfaces of additive manufacturing and its facets. A roadmap and standardization have been made available to existing specifications and standards. Within including the Design, Process Control, Materials and Machinery and several applications. These applications can be included as far as the Biomedical industry, Aerospace and Military to name a

few. Powder Bed Fusion is available for a metal material approach a type in the seven-category system in additive manufacturing. This category consists of several systems that can be utilized and each provides benefits for different specifications. This includes (SLS) Selective Laser Sintering, (SLM) Selective Laser Melting, (DMLS), Direct Laser Sintering, and (EBM) Electron Beam Melting. The main energy source of these divisions are: laser, electron beam or plasma arc. The process chain of Powder Bed Fusion is the preparation of the powder including examining and mixing, loading the material into the machine, sintering or melting of the powder, removing remaining and excess powder and finally submitting part for post processing.

There a total of six denominated shapes in which they are commercially available and currently utilized between this branch. The most commonly used are spherical, spheroidal and a combination of the previous two with the addition of satellites. This method operates with one or more sources of thermal energy for the powder particles to fuse. By controlling and selectively fusing material, powder bed is also capable of adding and recycling excess powder. Included in sintering, there are four types of fusing mechanisms that are present in powder bed fusion: Full melting chemically- induced binding, solid-State sintering, and liquid-phase sintering.

3.1.1 Types of Melting

Full Melting- the process in which a complete region of powder or material being used is subjected to imposing energy. Followed by then melting the material until the layer solidifies. In the powder layer thickness, a source of thermal energy (commonly electron beam or laser) is added until the final solidified part is fused.

Chemically-Induced Biding- Method in which chemical reactions are triggered through the use of thermal energy. In order to fuse the powder together the use of atmospheric gases and a

combination of two powders forms a by-product. Commonly used in ceramics and can as well produce exothermic reactions when administered with a laser.

Solid-State Sintering- Meaning fusing powder particles without the necessity of high temperatures involved, a mechanism that is principally used for diffusion. Considering only capturing half of the melting point temperature.

Liquid-Phase Sintering- The process of combining or coalescing powder particles whereby an assortment of particles turned out to be molten (glued). In this case some of the sections continue being solidified.

Upon these branches in Powder bed fusion two of the categories mentioned above are commonly used in industry, Electron beam Melting and Selective Laser Melting. Both of these are viable and sum numerous advantages since they are capable of creating channels and cavities. These two systems correlate to the additive manufacturing proficiencies in which they create intricate geometries. Both cases of manufacturing and fusing powder utilize the melting of the powder in its totality until layer is completely solidified. In the following paragraphs a closer look of the two methods are being analyzed and looked in depth.

3.2 Published Work

Overall there are numerous advantages mentioned throughout this work and further research documents published. Considerable advantages are presented, but continuous research efforts still focus to perfect this process and reduce limitations in printed material. Some of the main concerns that have been present throughout the practice of this method are the porosity present in a part, residual stresses and imperfections. This however provide a limitation curve in which cracks on tensile areas are found and provoke residual stresses to be present around the

printed model. As a consequence of cracking and defects, they can lower the resistance of loads being applied. Ongoing efforts have been made in order to understand, predict, and control the amount of residual stresses. Some of the findings of academia is that stresses can be focused and located perpendicular to the direction of the part being built. Post treatments are essential for elements to be submitted, this is to enhance and increase the materials mechanical properties. In this case a more in-depth explanation of why this occurs because the material is in direct exposure to thermal energy or heat transfer. If the presence of heat transfer, a thermal gradient will occur leading to thermal expansion of the particle, and the consequences of this generates thermal stress. This also remain in the part inside the material and after cooling down until reaching the temperature of its surroundings. Not only this are generated within the part, but as well they can contain of different sizes that the need for classification them is required. They are categorized and vary from the location of the part and the size. Type I residual stresses focus on considerable and extensive lengths; however, type II and type III may occur in the in the change and difference of the phases. More clearly defined, they develop due to dislocations at an atomic scale. This can cause problems since it creates deformations and lower its mechanical strength. In addition to external loads placed upon this cooled and solidified, external loads are added within internal stresses accumulated by thermally developed stresses. With a reduced strength cracks are more likely to propagate and lengthen from the surface.

The strength of the material aids all the heat and temperature induced in particles, this results in the prevention and continued by lowering the temperature. As formerly specified compressive stresses develop due to the thermal expansion created in which layers of material are confined. The material undergoes a shrinking mechanism and a bending angle is created while the laser progresses. Another considerable method that the material undergoes and creates the effect of

residual stresses is the phase where the particles cool down. Involving molten particle layers a residual stress emerge and take place in the material. Molten top layers react, and a shrinkage due to thermal tensile force of the bottom material and compressive stress arise in the primary top layers.

Some exhaustive testing has been ongoing in order to predict this behaviors and studies have a focus through testing of specimens. Comparing results of a test of Aluminum which in conjunction with the result of residual stresses a level of porosity have been present in specimens. Aluminum porosity is often present and a concerning theme by being one of the higher challenges by SLM caused when parts are in the solidifications stage. These are due to water vapor and/or any exposure to hydrogen material. As aluminum becomes molten it requires a high Hydrogen solubility limit that is present that must extenuate during this stage.

Some of the approaches considered are needed to help research and studies to determine some of the prevention methods for these effects caused. Papers have published a series of tests with the modification of certain print parameters to analyze the effect in the resulting challenges. A comparison was made by the University of Texas at Austin in 2014 with ALSI10MG and Aluminum 6061 by determining the main three challenges previously stated. This study conveys 5 different parameters in which they examine in both material as well as for Al 6061 whom a second test was completed. These 5 parameters were considered as the main focal points: Laser power, scan speed, scan spacing, layer thickness, and platform temperature [14]. The parameters previously mentioned are a main key in how a material can behave. In several research documents same constraints are utilized and modified. Aluminum is commonly used and by the adjustments mentioned it can reduce the percentage of imperfections frequently seen.

The tested material originally presented portrays imagines of iterations performed shown below. Depicting the varying outcome difference of applying different power, speed and even cracking and porosity depending on the axis of built taken.

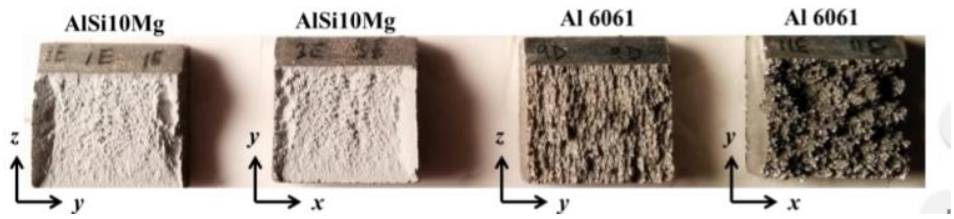

Figure 21: Metal orientation comparison[10]

From several experimental studies exact observations of the specimens were created and could be analyzed in depth. From the numerical standpoint it can be denoted that the furthermost achievements can be made by prediction and prevention of this cases. We can observe Nanyang published work by simulating an FE model utilizing the governing heat transfer equations for a nonlinear transient process. For this purpose, two phases are considered to be tested: from solid to liquid and vice versa, taking into the account of the thermophysical properties as the central factors. Some of the difficulties in the numerical methods are added for which constructing a simulation of phase changes is rather complicated. In this study case it is presented as a volume shrinkage and is identified as volume ratio where the change in volume and heat exchange are collected. As aforementioned the ratio of the volume between the molten volume of the powder to the material removed by vaporization in which it denominates a focus on the metal pool created and solidification of the part. In between these processes utilizing the numerical method approached, it produces results that could be related to the actual experimental analysis performed. Indicating several width measurements and melt penetrations, each within the distance of the scanning laser. As they present three denominations named as “HH” “LH” “LL”, of 1.3 ratio (41.7-140.3 um) a ratio of 1.25 (22.9.99.5 um) and 1.33 (33.-130.6 um) respectively.

Each case with the designated laser speed of 300 mm/s with a closer look at t being .001 reaching steady state utilizing a 50 µm powder. A laser spot size of 80 µm and designating the laser power varying from 150 to 350 W with an interval of 100W. Resulting information led to a conclusion of the success of simulating strategies correlating to an experimental approach.

Test #2		Power (W)				
		370	345	320	295	270
Speed (mm/s)	1500	Z	Z	Y	Y	Y
	1250	Z	Z	R	R	Y
	1000	A	R	R	R	R
	750	A	A	A	A	R
	500	A	A	A	A	A

Figure 22: Testing parameters of laser speed [10]

These experimental studies are brought upon the work of this paper for the whole purpose of deeply understanding the variants previously performed for similar cases for this research.

We can take note as in this specific study the results are fore most advantageous. However, investigating the same parameters without the cost and extenuating waste of resources by performing finite element models can become more beneficial. The main purpose of this presented work is to facilitate investigation of particles, by recurring to an analysis in which parameters could be modified and simulated. Ultimate goal is to compose of simple validation models to corroborate the theory behind the analysis taking with the following governing equations.

As a start for this research a set of properties were obtained from “Properties of Aluminum Alloys: Tensile, Creep, and Fatigue Data at High and Low Temperatures”, J. Gilbert Kaufman. These properties were extracted from the tensile section of Aluminum 6061 and were analyzed in

different temperatures by then validating them through a FE model in Abaqus. Mechanical properties throughout time such as tensile, yield strengths, elongation percentage and modulus of elasticity are listed with respect through time. For the most part the expectations of these properties will predict a declination of limits as the temperatures rise. This assumption is made since Aluminum metal loses its mechanical properties as it continuously rises in temperature and reaches its melting point. This will follow by a validation test utilizing a modeling software ABAQUS. The ASTM E8/E8M Standard Test Methods of Tension Testing of Metallic Materials with standard specimen dimensions for metals was used.

Yield and tensile stresses were graphed for comparison, this is mainly shown in order to give a visual representation of the different behaviors in the mechanical properties as temperature increases. A strain- stress curve is projected with each temperature set with different colors and as temperature rises tensile and yield stress decreases.

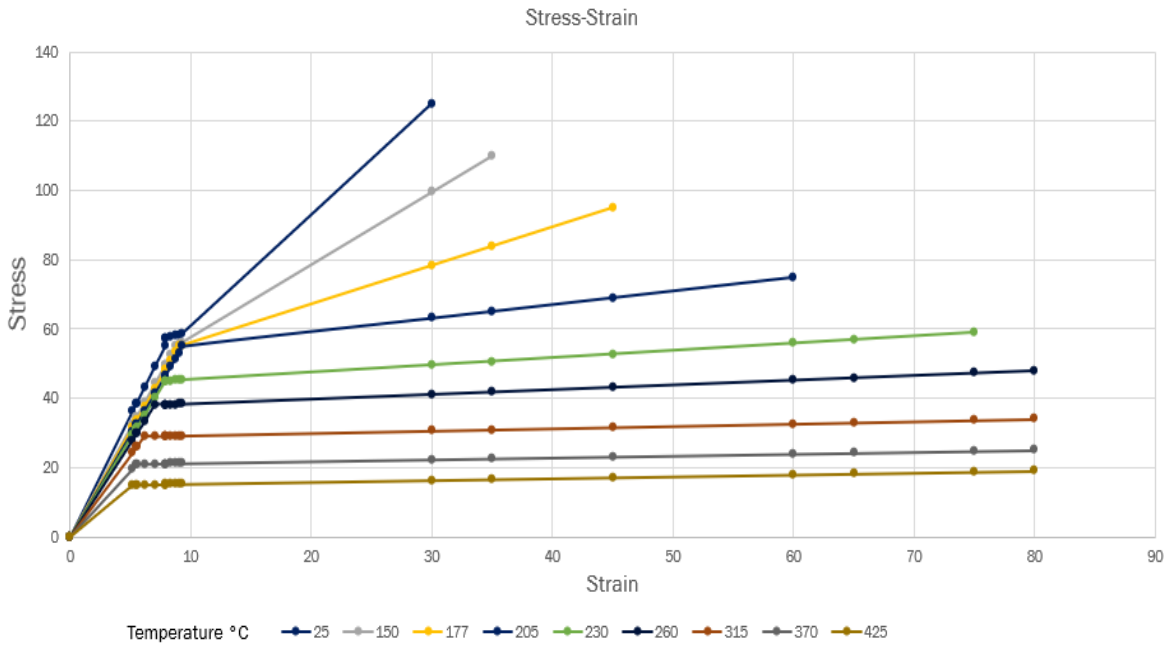

Figure 23: Stress-Strain curve at different temperatures.

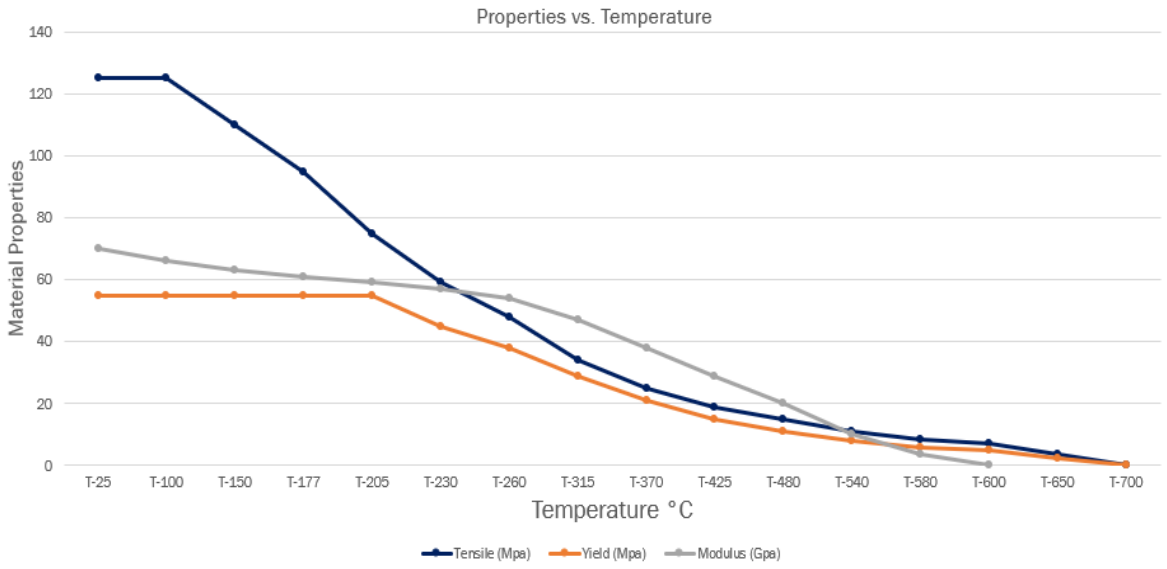

Figure 24: Graphed properties through temperature from yielding point

As shown in figure 25 a plate type of 40 mm (1.5in) wide dimensions was modeled with a thickness maximum of 5 mm (0.188in) [10]. As the main focus of this test was to complete and analyze tensile and yield stresses. Finally, a comparison of the information obtained with the published documentation was performed with a ¼ symmetry of the specimen shown.

E8/E8M – 16a

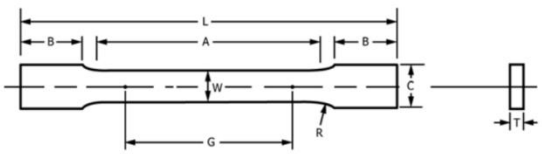

	Dimensions		
	Standard Specimens		Subsize Specimen
	Plate-Type, 40 mm [1.500 in.] Wide	Sheet-Type, 12.5 mm [0.500 in.] Wide	6 mm [0.250 in.] Wide
	mm [in.]	mm [in.]	mm [in.]
G—Gauge length (Note 1 and Note 2)	200.0 ± 0.2 [8.00 ± 0.01]	50.0 ± 0.1 [2.000 ± 0.005]	25.0 ± 0.1 [1.000 ± 0.003]
W—Width (Note 3 and Note 4)	40.0 ± 2.0 [1.500 ± 0.125, -0.250]	12.5 ± 0.2 [0.500 ± 0.010]	6.0 ± 0.1 [0.250 ± 0.005]
T—Thickness (Note 5)		thickness of material	
R—Radius of fillet, min (Note 6)	25 [1]	12.5 [0.500]	6 [0.250]
L—Overall length, min (Note 2, Note 7, and Note 8)	450 [18]	200 [8]	100 [4]
A—Length of reduced parallel section, min	225 [9]	57 [2.25]	32 [1.25]
B—Length of grip section, min (Note 9)	75 [3]	50 [2]	30 [1.25]
C—Width of grip section, approximate (Note 4 and Note 9)	50 [2]	20 [0.750]	10 [0.375]

Figure 25: Dimensions for necking specimens in metals.[11]

3.3 Modeling

This specimen was modeled with dimensions of 225 mm [8.85in] of length, with a cross-sectional area of 25mm x 2.5 mm in grip section and 20mm x 2.5 mm of cross-sectional area in the test section (necking area). Some of the conditions applied for the specimen to comply with the ASTM required dimensioning an X, Y and Z symmetry selections were made. Testing of two points of necking part of the model with a starting set temperature of 205 C was tested.

Table 4: Prototype dimensions

Length (L)	225 mm
Width of Grip Section (C)	25 mm
Width (W)	20 mm
Thickness (T)	2.5 mm

These measurements were developed according to the ASTM Standard Test Methods for Tension Testing of Metallic Materials. The reason for considering these dimensions was to ultimately apply the model into tensile testing in finite element analysis in Aluminum 6061. A set of two iteration were made with the same geometry following a dog-bone like model. These were made not following any specific dimensions. Followed by these iterations a final model was made with the ASTM specifications previously mentioned.

Table 5: Abaqus input properties from Al 6061 at 215Cº.

Density	2.7x10^-9	g/cm^3
Young´s Modulus	59	GPa
Poison´s Ratio	0.33	Unitless
Elongation Percentage	60	Percentage

Material named Aluminum was created to model the mechanical properties and its material behaviors. Mass density was set to 2.7E-009, mechanical elasticity was also considered including Young's Modulus of 59GPa and Poisson's Ratio of 0.33 and 60% elongation as laid out in the table below.

As part of determining the load that the material is going to be tested in some of the most basic equations are going to be used. Since we know the yield stress of 55MPa, the tensile stress of 75MPa and the modulus of elasticity 59MPa we can determine the strain stress. For that we can proceed to use:

$$\epsilon = \frac{\delta_{yield}}{E} \rightarrow \in = \frac{55\ MPa}{59{,}000 MPa} = 9.322x10^{-4} \qquad \text{equation. (7)}$$

We can now use this result of 9.322E-4 to subtract it to the elongation percentage for the purpose of obtaining the original strain starting from the yield point of the curve where plasticity begins.

$$60\%\ \text{elongation} - \text{Strain}_{yield} \qquad \text{equation. (8)}$$

0.6- 9.322E-4=0.59906

The obtained result will be entered in Abaqus plastic card that records the point where the yielding starts. Followed by the set of points previously obtained a load must be determined for the test section and the grips section to use it as an input in Abaqus and validate results from Kaufman.

Load on both sections can be obtained by the simple equation utilizing the yield stress and the area of the grip and the test sections.

Load for test section:

$$P_{yield} = \delta_{yield} \cdot A_{test} \qquad \text{equation. (9)}$$

$$P_{yield} = (\ 55\ \text{MPa})(50mm^2) = 2750\ N$$

Traction on grip:

$$\tau_{grip} = \frac{P_{yield}}{A_{grip}} \qquad \text{equation. (10)}$$

$$\tau_{grip} = \frac{2750\ N}{62.5\ mm^2} = 44$$

Traction with ultimate tensile stress

$$\tau_{UTS} = (75MPa) \cdot (\frac{50mm^2}{62.5\ mm^2}) = 60 \qquad \text{equation. (11)}$$

A 2 by 2 matrix with the yield stress and plastic strain was also applied with a time period of 240. As part of the boundary conditions an amplitude selection was also made to match the time periods. For this test with a load of 52MPa for the traction on top part of the model was set to simulate the tensile testing.

Data

	Yield Stress	Plastic Strain
1	55	0
2	75	0.5992

Name: Amp-1
Type: Tabular
Time span: Step time
Smoothing: Use solver default
Specify:
Amplitude Data | Baseline Correction

	Time/Frequency	Amplitude
1	0	0
2	240	1

Figure 26: Amplitude data selected & Plastic properties

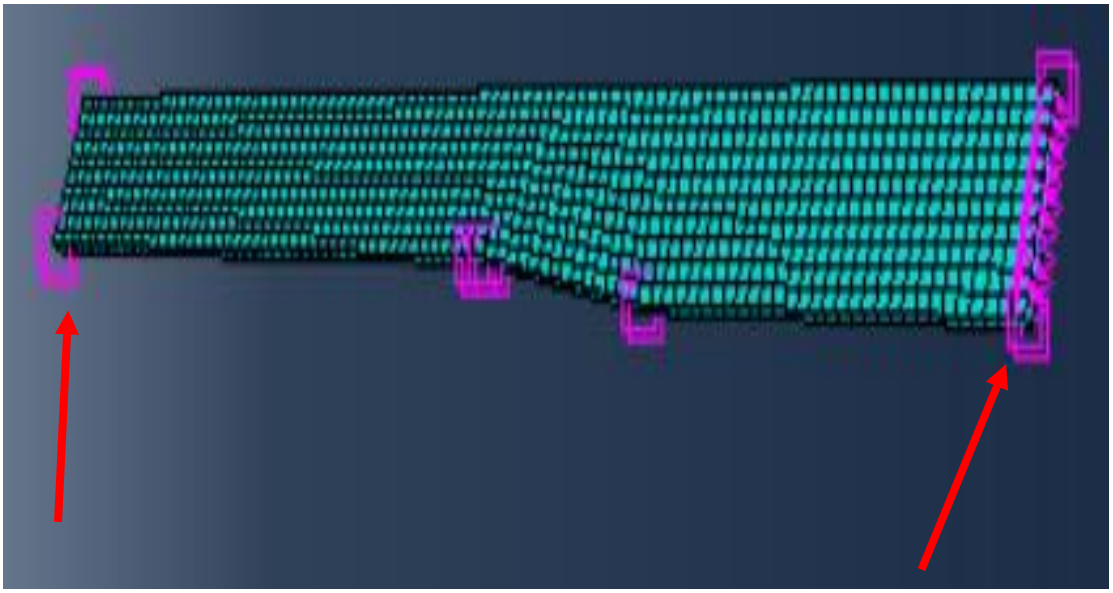

Figure 27: Meshing on prototype

3.4 Boundary Conditions

As shown on figure 27, one of the main steps into obtaining results from Abaqus is meshing the part according to the required detail of results. For this prototype size of the mesh is not as relevant as if you are simulating the actual laser diameter for example. Since this is a simple tensile test even meshing on each corner line of the prototype is set to a global size of 11. As well as a minimum size control is set to be a fraction of the global size as 0.1 from in between a set parameter of 0.0 < min < 1.0 as shown in figure 28. Geometry can also be modified to select a specific type of meshing and depending on the focus point of the specimen a certain geometry can be stated. For this test simple general squares were selected.

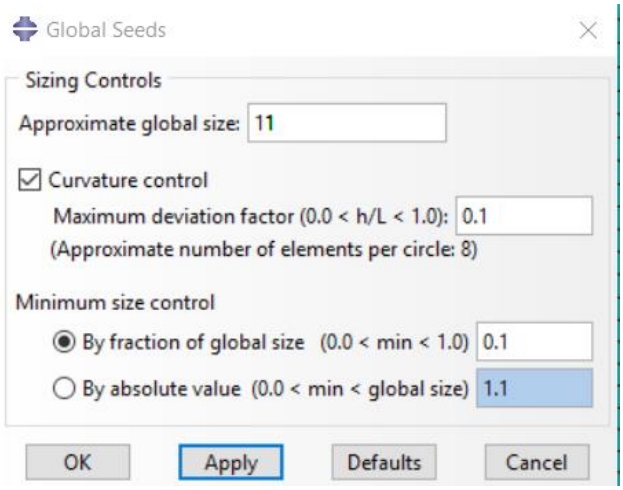

Figure 28: Meshing parameters

In order to obtain and perform a correct stress-strain curve we could extract data from the visualization of the results obtained in Abaqus. An XY Data will be extracted from the active frames from a requested ODB Field Output which will show XY Data output. This is performed by selecting a unique nodal from the output variables shown. Upon selecting the unique nodal option for this test, we are only interested in U2 which is the Y symmetry selection of the spatial displacement. Nodes can be selected by several forms, such as picking from the viewport,

selecting labels sets and internal set previously created. In this case the nodes were selected picking from the viewport individually (total of 2 nodes).

By this a selection can be made by choosing the number of nodes directly from the meshed model as shown in figure 29 below. The points were selected randomly with the mere intention of recording a set original distance from node to node in the necking area. This is to have an original length by later comparing it to the deformation caused by the load applied in each temperature being tested. Meaning that the nodes were a part of the testing area (necking) were the load applied can be more affected and cause mayor stress compared to other sections of the model, such as the grip section.

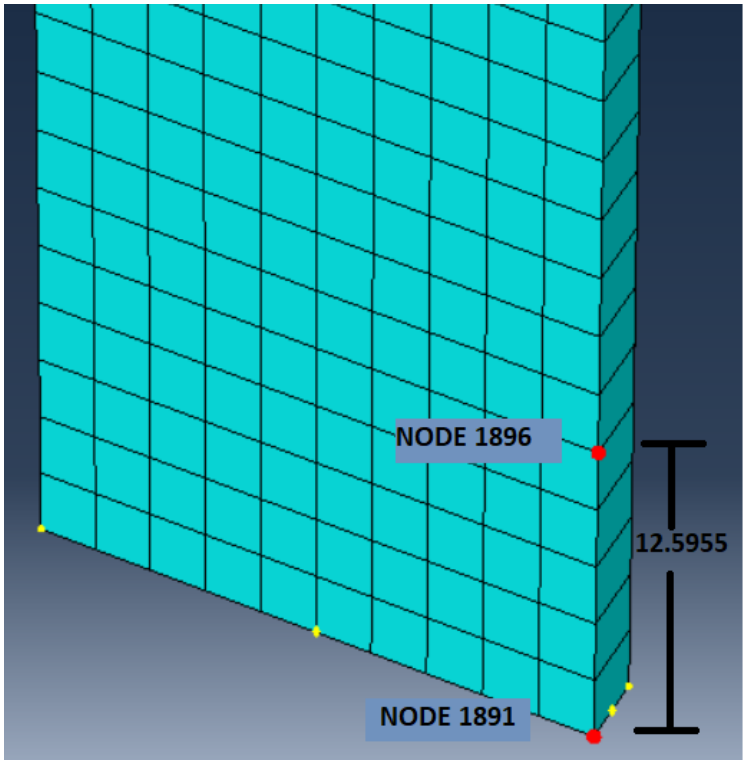

Figure 29: Node location with total distance in between (Lo).

Node 1891 and 1896 was selected and a list is given by Abaqus with respect to the step selected. In this case data is pulled every 0.5 second until it reaches a total of 240 as formerly selected.

Once nodes are selected and the ODB Field Output saved, the “Edit” option is selected to obtain an excel table with the data that can now be transferred into an Excel sheet which will allow a much easier manipulation of the data obtained. This data is compiled, and a set of basic equations are utilized to create a chart of the Abaqus output data versus the Kauffman’s data. This simple example can validate the data obtained.

Edit XY Data

Name: U:U2 PI: TEST-1 N: 1896

	X	Y
1	0	0
2	0.5	3.05771E-005
3	1	6.11543E-005
4	1.75	0.00010702
5	2.75	0.000168174
6	3.75	0.000229328
7	4.75	0.000290483
8	5.75	0.000351637
9	6.75	0.000412791
10	7.75	0.000473945
11	8.75	0.0005351
12	9.75	0.000596254
13	10.75	0.000657408
14	11.75	0.000718562
15	12.75	0.000779717
16	13.75	0.000840871
17	14.75	0.000902025
18	15.75	0.00096318
19	16.75	0.00102433
20	17.75	0.00108549
21	18.75	0.00114664
22	19.75	0.0012078
23	20.75	0.00126895
24	21.75	0.00133011
25	22.75	0.00139126
26	23.75	0.00145241
27	24.75	0.00151357
28	25.75	0.00157472
29	26.75	0.00163588
30	27.75	0.00169703

Figure 30: XY Node Data extracted

3.5 Testing and Results

The general equations utilized are repeated throughout both tests. Obtaining the Step determined information, both nodes (1891 and 1896), original length (Lo), force, stress and strain are necessary to obtain the validation.

With this information we can now calculate the stress-strain curve. The results of these test complied with the expected results and a stress-strain graphs were also obtained to validate the properties. This test was repeated for at least 3 set temperatures for comparison and validation purposes.

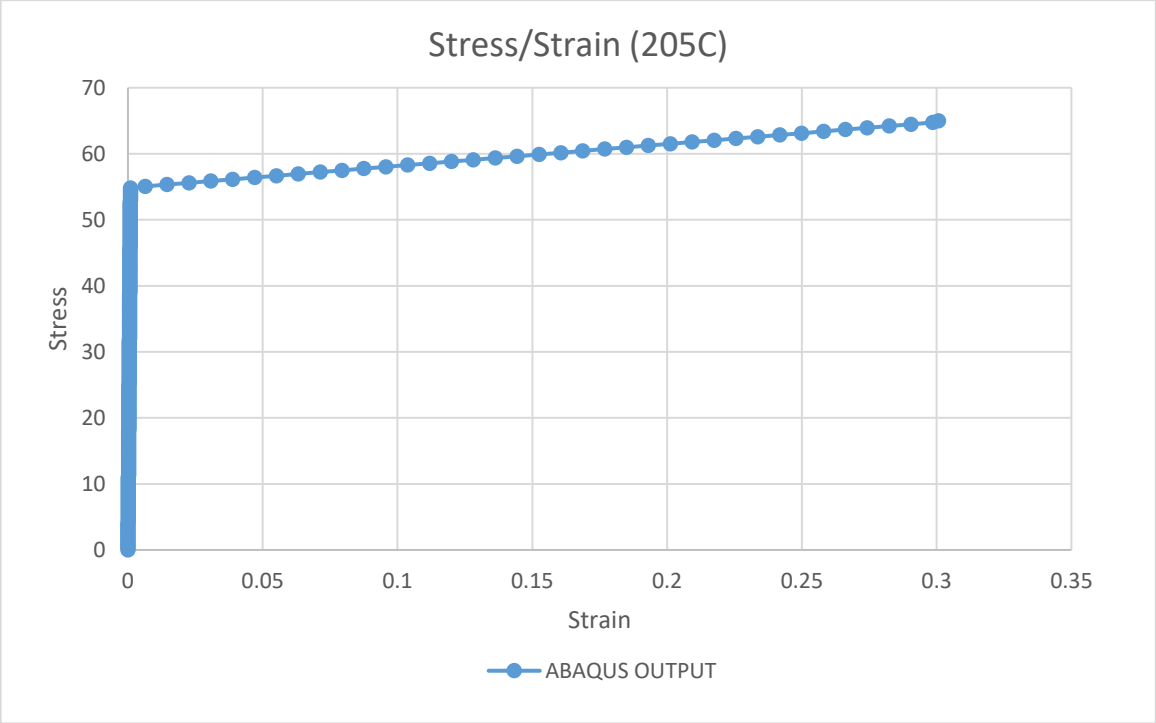

Figure 31: Stress-Strain Abaqus output curve.

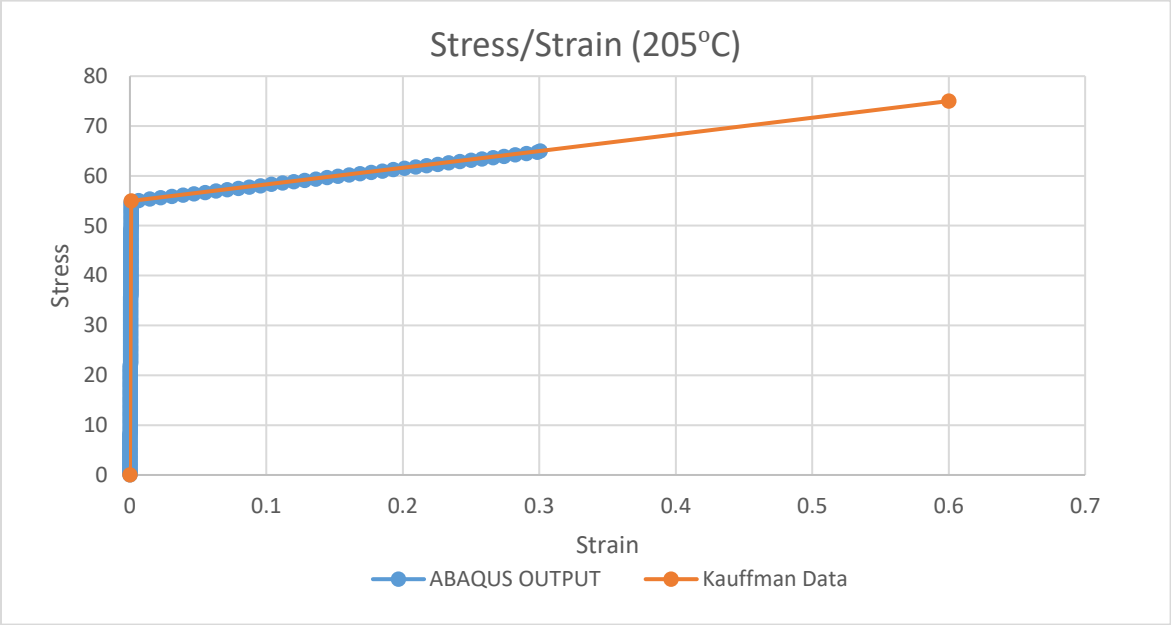

Figure 32: Abaqus Output vs. Kauffman Data (205°C)

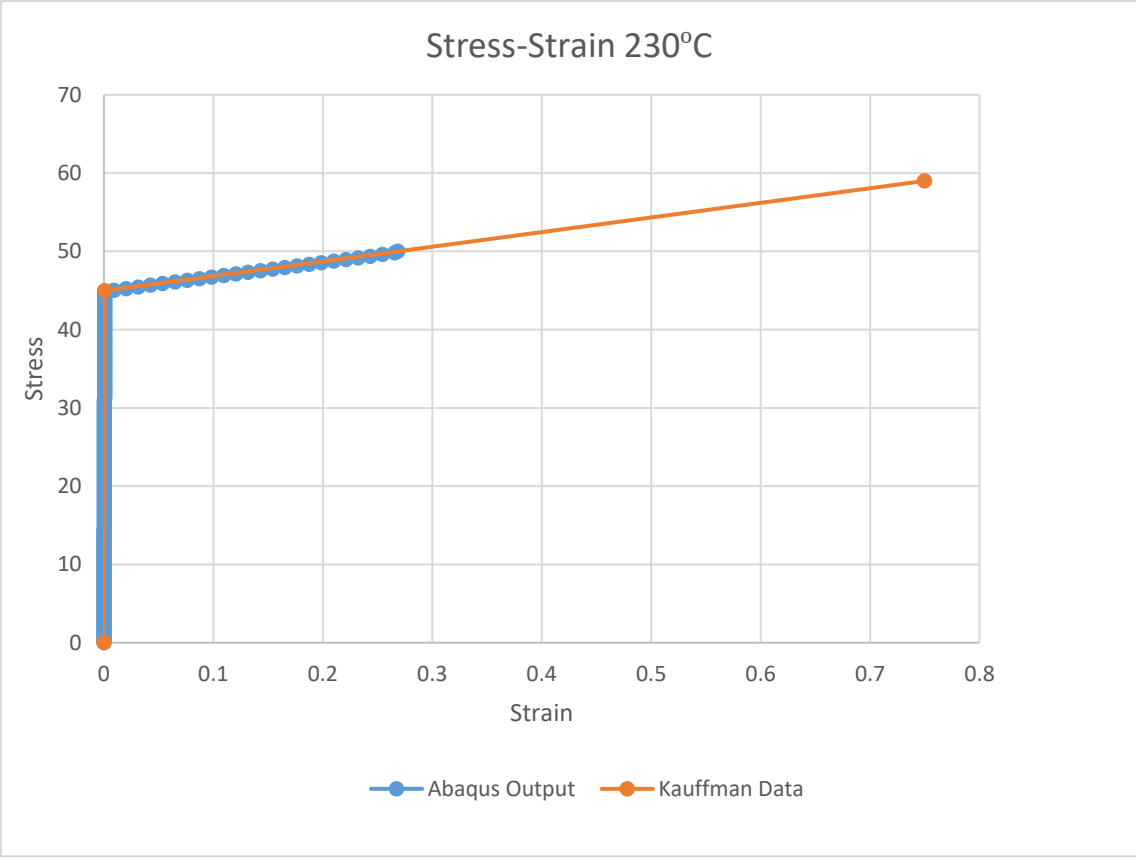

Figure 33: Abaqus Output vs. Kauffman Data (230°C)

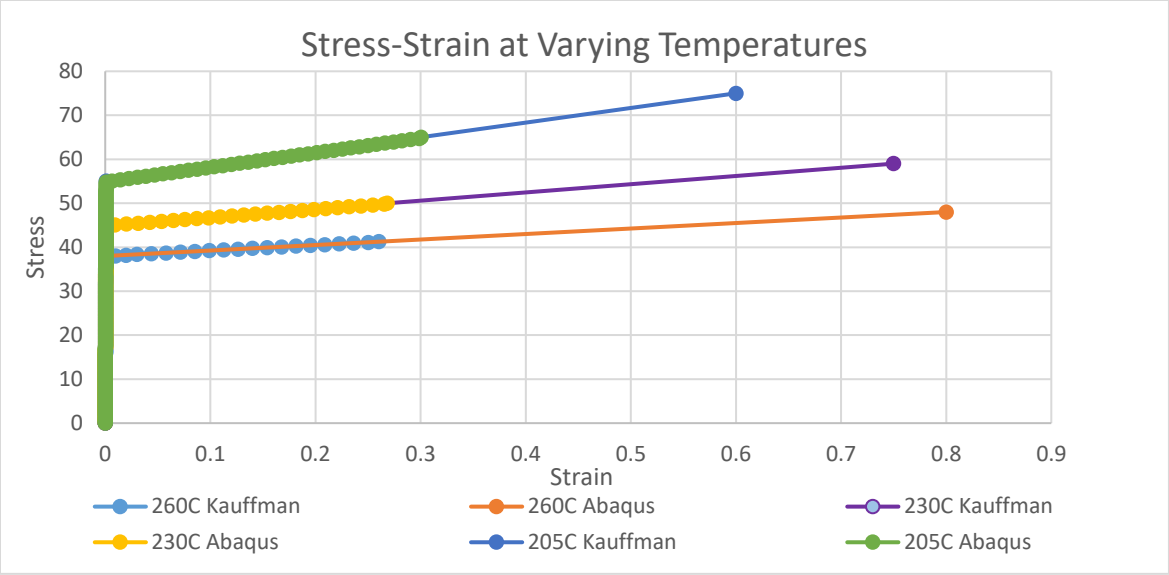

Figure 34: Stress-Strain curve at varying temperatures

From figure 32, the graph can illustrate the point in which the material reaches yield at 55MPa which correlates with the published work. For this model with a temperature of 205C the traction load was set to 52MPa as formerly mentioned, by the compared results Abaqus and book data are completely the same. Dotted lines shown in the graph were enabled to mark the comparison between both of the information obtained. As it is seen this data reaches to a certain point, this is due to the fact that Abaqus traction load is set to a specific calculated load. This load is reaching into fracture or the ultimate tensile stress.) We can come into a conclusion that the data is validated throughout this simplified example.

This procedure is repeated three more times with the same followed procedure to verify the data obtained. These additional tests were made using different temperatures and the recorded mechanical properties for each temperature. Along with the temperatures the same basic equations utilizing the mechanical properties extracted from publications and compared to Abaqus output.

Chapter 4: Conclusion

In conclusion, the purpose of this work is to inform and analyze additive manufacturing methods such as SLM with Aluminum 6061-O and FDM with PLA. With this accomplishing some validation examples of data previously obtained from Kauffman. A ¼ symmetric test specimen was modeled in Abaqus implementing boundary conditions and traction loads in order to simulate a tensile test. Dimensions were modeled from the ASTM regulations for tensile testing of metals. As well as previously shown the model was set to several temperatures and three of them were recorded with its respective data for each of them. The comparison was made between the simulation and the data from published work. Output data from Abaqus was used into some basic formulas such as stress over strain and normalizing the information obtain a correct set of information. Followed by finally comparing both of the data and validating with success the material. Some other published work was mentioned with the purpose of investigating deeply some of the main reasons of why imperfections occur in SLM. These were stated to be the focus of this work presented for the intention of investigating parameters that could later determine a solution. Porosity and cracking on the specimens is commonly seen, as some parameters have been specified, validated work on this paper shows the first step into a deeper investigation of this issue. The intended purpose is to follow a path of researching and creating validation examples utilizing finite element analysis and followed by testing specimens. For FDM research PLA and steel properties were introduces in order to simulate a model filament and nozzle in ME. For this the material was introduced to two tests to research material behavior. First test was concluded with the stress and flow of the filament with a result of minimal movement. For the second test, inputs were added including the displacement of PLA, as well as volumetric compliance data. This resulted in higher flow of the material as predicted

and considered to be validated. Purpose of the second test was to obtain a higher flow to simulate test originally recorded.

Chapter 5: Future Work

In the investigation and analysis of additive manufacturing an example was presented as mentioned and shown in this work. Future work is meant to be performed continuing with the execution of some simulations with the laser utilized in SLM. Prototypes and Fortran subroutines are also seen in Abaqus trying to set a certain path for the laser to follow in a specimen. This can be simulated since there is some work presented showing the advances and explanation of how these parameters can help reduces porosity and other imperfections occurring in specimens. Followed by further testing the material and observing PLA upon creeping testing. Steps have been planes such as creating a dog-bone like structure to facilitate creeping and relaxation further testing. Viscoelasticity will also be a future focus into detailing the research in a phase change perspective. Raster pattern and print induced defects are also issues that are often seen as a possible research defect due to its repeated rupture pattern.

References

[1] “Hybrid Manufacturing Resources.” Hybrid Manufacturing Technologies, 2015, www.hybridmanutech.com/resources.html.

[2] Terrazas, C., W.M. Keck Center., (2016). Extrusion-Based Systems.

[3] America Makes, ANSI Additive Manufacturing Standardization Collaborative, (2017). Standardization Roadmap for Additive Manufacturing, Version 1.0.

[4] Shah, K. P., Fatigue Test and Creep Test.

[5] ASTM E139-11(2018) Standard Test Methods for Conducting Creep, Creep-Rupture, and Stress-Rupture Tests of Metallic Materials, ASTM International, West Conshohocken, PA, 2018, https://doi.org/10.1520/E0139-11R18

[6] Conci, P., (2016). 3D Printer Smart Nozzle. https://contest.techbriefs.com/2016/entries/machinery-automation-robotics/7080

[7] Mashayeki., Adaptive Meshing
https://mashayekhi.iut.ac.ir/sites/mashayekhi.iut.ac.ir/files//u32/presentation8.pdf

[8] Malkin. Y. A., Isayev, I. A., (2012). Viscoelasticity. Rheology Concepts, Methods, and Applications (Second Edition).

[9] Palermo, E., (2013). What its Selective Laser Sintering.
https://www.livescience.com/38862-selective-laser-sintering.html

[10] Fulcher, B. A., Leigh, D. K., & Watt, T. J. COMPARISON OF ALSI10MG AND AL 6061 PROCESSED THROUGH DMLS.

[11] ASTM E8/E8M-13 Standard Test Methods for Tension Testing of Metallic Materials, ASTM International, West Conshohocken, PA, 2013, https://doi.org/10.1520/E0008_E0008M-13

[12] Roylance, D. (2001). Engineering Viscoelasticity. Massachusetts Institute of Technology.

[13] Mashayeki., Adaptive Meshing
https://mashayekhi.iut.ac.ir/sites/mashayekhi.iut.ac.ir/files//u32/presentation8.pdf

[14] Malkin. Y. A., Isayev, I. A., (2012). Viscoelasticity

[15] Rezgui, F., Swistek, M., Hiver, J. M., G'sell, C., & Sadoun, T. (2005). Deformation and damage upon stretching of degradable polymers (PLA and PCL). Polymer, 46(18), 7370-7385.

[16] Gaders, Gene. (2000). Creep and Creep Testing.

[17] Fuhrman, K., Zheng, W., (2017). CREEP AND RECOVERY OF POLYLACTIC ACID AND ITS CLAY NANOCOMPOSITE.

[18] Nikhil, A. 3D Printing Processes- Material Extrusion (Part 2/8), https://www.engineersgarage.com/articles/3d-printing-processes-material-extrusion

[19] Donovan, R., Fortune, R., & Trout, R. (2015). Elevated Temperature Effects on the Mechanical Properties of Age Hardened 6xxx Series Aluminum Alloy Extrusions.

[20] Liu, K., Ovaert, C. T., (2011). Poro-viscoelastic constitutive modeling of unconfined creep of hydrogels using finite element analysis with integrated optimization method.

[21] Trevisan, F., Calignano, F., Lorusso, M., Pakkanen, J., Aversa, A., Ambrosio, E. P., Lombardi, M., Fino, P., … Manfredi, D. (2017). On the Selective Laser Melting (SLM) of the AlSi10Mg Alloy: Process, Microstructure, and Mechanical Properties. Materials (Basel, Switzerland), 10(1), 76. doi:10.3390/ma10010076

[22] Benedyk, C. J., (2018). Additive Manufacturing of Aluminum Alloys.

[23] Frazier, W.E. J. of Materi Eng and Perform (2014) 23: 1917. https://doi.org/10.1007/s11665-014-0958-z

[24] Majinder, S., SC16M072 (2017). Indian Institute of Space Science and Technology BULK METALLIC GLASSES

[25] Findley, W. N., & Lai, J. S. Y. (1967). A modified superposition principle applied to creep of nonlinear viscoelastic material under abrupt changes in state of combined stress. Transactions of the Society of Rheology, 11(3), 361-380.

[26] SLM Solutions., Company History. https://slm-solutions.com/about-slm/company-history

[27] Elservier. B. V., Dong. L., Makradi, S. A., Remond, Y., (2008). Three-dimensional transient finite element analysis of the selective laser sintering process.

[28] Mauduit, Arnold. (2017). Study of the suitability of aluminum alloys for additive manufacturing by laser powder bed fusion. UPB Scientific Bulletin, Series B: Chemistry and Materials Science. 79. 219 - 238.

[29] Zaeh, M.F. & Branner, G. Prod. Eng. Res. Devel. (2010) 4: 35. https://doi.org/10.1007/s11740-009-0192-y

[30] Salmi. A., Atzeni, E., Luliano, L., Galati, M., (2015-1017). Experimental Analysis of Residual on AlSi10Mg Parts Produced by Means of Selective Laser Melting (SLM).

[31] Protasov, C. E., Safronov, V. A., Kotoban, D. V., Gusarov, A. V. (2016). Experimental Study of Resudial Stresses in Metal Parts Obtaned by Selective Laser Melting.

[32] Peter Mercelis, Jean-Pierre Kruth, (2006) "Residual stresses in selective laser sintering and selective laser melting", Rapid Prototyping Journal, Vol. 12 Issue: 5, pp.254-265,https://doi.org/10.1108/13552540610707013

[33] Castells, R., (2016). DMLS vs SLM 3D Printing for Metal Manufacturing. https://www.element.com/nucleus/2016/06/29/dmls-vs-slm-3d-printing-for-metal-manufacturing

[34] Alcoa Engineered Products., (2002). Understanding Extrude Aluminum Alloys.

[35] Shiomi, M., Osakada, K., Nakamura, K., Yamashita, T., & Abe, F. (2004). Residual stress within metallic model made by selective laser melting process. *CIRP Annals-Manufacturing Technology*, *53*(1), 195-198.

Appendix A- Abaqus Input Files

Input File A-1

```
*Heading
 *Heading
** Job name: test1 Model name: Model-1
** Generated by: Abaqus/CAE 2017
*Preprint, echo=NO, model=NO, history=NO, contact=NO
**
** PARTS
**
*Part, name=Filament
*Node
*Nset, nset=_PickedSet2, internal, generate
  1,  820,    1
*Elset, elset=_PickedSet2, internal, generate
  1,  696,    1
** Section: Filament
*Solid Section, elset=_PickedSet2, material=Filament
1.,
*End Part
**
*Part, name=Nozzle
*Node
*Element, type=CAX3T
*Nset, nset=_PickedSet2, internal, generate
  1,  811,    1
*Elset, elset=_PickedSet2, internal, generate
  1,  704,    1
** Section: Nozzle
*Solid Section, elset=_PickedSet2, material=Steel
1.,
*End Part
**
**
** ASSEMBLY
**
*Assembly, name=Assembly
**
*Instance, name=Nozzle-1, part=Nozzle
*End Instance
**
*Instance, name=Filament-1, part=Filament
        0.,    -0.259777,           0.
*End Instance
**
```

```
*Nset, nset=_PickedSet24, internal, instance=Nozzle-1
  24,  25, 170
*Elset, elset=_PickedSet24, internal, instance=Nozzle-1
 146, 240
*Nset, nset=_PickedSet25, internal, instance=Filament-1, generate
   1,  820,    1
*Elset, elset=_PickedSet25, internal, instance=Filament-1, generate
   1,  696,    1
*Nset, nset=_PickedSet26, internal, instance=Nozzle-1, generate
   1,  811,    1
*Nset, nset=_PickedSet26, internal, instance=Filament-1, generate
   1,  820,    1
*Elset, elset=_PickedSet26, internal, instance=Nozzle-1, generate
   1,  704,    1
*Elset, elset=_PickedSet26, internal, instance=Filament-1, generate
   1,  696,    1
*Elset, elset="_filament contact surf_S4", internal, instance=Filament-1
  39,  53,  54,  55,  56,  57,  58,  59,  60,  61,  62,  63,  64,  65,  66,  67
  68,  69,  70, 136, 137, 140, 150, 152, 156, 164, 165, 166, 167, 168, 169, 170
 171, 172, 174, 175, 176, 177, 178, 179, 180, 181, 182, 183, 184, 185, 186, 187
 188, 189, 190, 191, 192, 193, 194, 195, 196, 197, 198, 199, 200, 201, 202, 203
 204, 205, 206, 207, 208, 209, 210, 211, 212, 213, 214, 215, 216, 217, 218, 219
 295,
*Elset, elset="_filament contact surf_S2", internal, instance=Filament-1
  48,  50,  51,  79,  80,  81,  82,  83, 134, 143, 153, 154, 155, 157, 160, 161
 162, 163, 220, 221, 289, 290, 302, 316, 330, 436, 675, 677, 678, 679, 687, 689
 690, 691
*Elset, elset="_filament contact surf_S3", internal, instance=Filament-1
  77,  84, 147, 148, 149, 173, 683
*Elset, elset="_filament contact surf_S1", internal, instance=Filament-1
  85,  86,  87,  88,  89, 142, 144, 145, 146
*Surface, type=ELEMENT, name="filament contact surf"
"_filament contact surf_S4", S4
"_filament contact surf_S2", S2
"_filament contact surf_S3", S3
"_filament contact surf_S1", S1
*Elset, elset="_nozzle contact surf_S1", internal, instance=Nozzle-1
  23,  24,  25,  26,  27, 152, 153, 154, 233, 269, 270, 271, 272, 275, 278, 279
 280, 281, 290, 292, 297, 314, 370
*Elset, elset="_nozzle contact surf_S3", internal, instance=Nozzle-1
 157, 161, 273, 274, 282, 283, 284, 285, 286, 287, 288, 289, 295, 321, 684
*Elset, elset="_nozzle contact surf_S4", internal, instance=Nozzle-1
 276,
*Surface, type=ELEMENT, name="nozzle contact surf"
"_nozzle contact surf_S1", S1
"_nozzle contact surf_S3", S3
```

```
"_nozzle contact surf_S4", S4
*Elset, elset=__PickedSurf22_S3, internal, instance=Filament-1
 46,
*Elset, elset=__PickedSurf22_S2, internal, instance=Filament-1
 89,
*Surface, type=ELEMENT, name=_PickedSurf22, internal
__PickedSurf22_S3, S3
__PickedSurf22_S2, S2
*Elset, elset=__PickedSurf23_S3, internal, instance=Nozzle-1
  16,  47,  51,  67,  76,  90,  99, 103, 104, 146, 235, 634, 662
*Elset, elset=__PickedSurf23_S4, internal, instance=Nozzle-1
  17,  35, 145, 238, 646, 663
*Elset, elset=__PickedSurf23_S1, internal, instance=Nozzle-1
  19,  42,  58,  94, 231, 234, 236, 237, 641, 664, 665, 666, 668
*Elset, elset=__PickedSurf23_S2, internal, instance=Nozzle-1
 106,
*Surface, type=ELEMENT, name=_PickedSurf23, internal
__PickedSurf23_S3, S3
__PickedSurf23_S4, S4
__PickedSurf23_S2, S2
__PickedSurf23_S1, S1
*End Assembly
*Amplitude, name="Ramp 2 sec"
           0.,           0.,           2.,           1.
**
** MATERIALS
**
*Material, name=Filament
*Conductivity
 0.21,
*Density
 9.7e-19,
*Elastic, moduli=LONG TERM
1000., 0.4
*Plastic
2.,0.
7.,2.
*Specific Heat
 1e+12,
*Viscoelastic, time=CREEP TEST DATA
*Volumetric Test Data, volinf=1.66
 9.047,62.
*Material, name=Steel
*Conductivity
43.,
*Density
```

```
 7.8e-12,
*Elastic
200000., 0.3
*Specific Heat
 5.02e+08,
**
** INTERACTION PROPERTIES
**
*Surface Interaction, name=ContactProp
1.,
*Friction, slip tolerance=0.005
 0.2,
*Surface Behavior, pressure-overclosure=HARD
**
** PREDEFINED FIELDS
**
** Name: Predefined Field-1   Type: Temperature
*Initial Conditions, type=TEMPERATURE
_PickedSet26, 100.
**
** INTERACTIONS
**
** Interaction: contact
*Contact Pair, interaction=ContactProp, type=SURFACE TO SURFACE
"filament contact surf", "nozzle contact surf"
** ----------------------------------------------------------------
**
** STEP: Adiabatic extrude
**
*Step, name="Adiabatic extrude", nlgeom=YES, inc=10000
*Coupled Temperature-displacement, creep=none, deltmx=50., stabilize, factor=0.0002,
allsdtol=0, continue=NO
0.001, 10., 1e-06, 0.01
*Solution Technique, type=SEPARATED
**
** BOUNDARY CONDITIONS
**
** Name: nozzle fixation Type: Displacement/Rotation
*Boundary
_PickedSet24, 2, 2
*Adaptive Mesh Controls, name=ALE mesh rule
1., 0.
*Adaptive Mesh, elset=_PickedSet25, controls=ALE mesh rule, op=NEW
**
** LOADS
**
```

```
** Name: Heat flux   Type: Surface heat flux
*Dsflux
_PickedSurf23, S, 1.
** Name: extrude pressure   Type: Pressure
*Dsload, amplitude="Ramp 2 sec"
_PickedSurf22, P, 0.07
**
** OUTPUT REQUESTS
**
*Restart, write, frequency=0
**
** FIELD OUTPUT: F-Output-1
**
*Output, field, variable=PRESELECT
**
** HISTORY OUTPUT: H-Output-1
**
*Output, history, variable=PRESELECT, frequency=5
*End Step
1
```

Input File A-2 Viscoelasticity

```
*Heading
** Job name: test1 Model name: Model-1
** Generated by: Abaqus/CAE 2017
*Preprint, echo=NO, model=NO, history=NO, contact=NO
**
** PARTS
**
*Part, name=Filament
*Node
*Element, type=CAX3T
*Nset, nset=_PickedSet2, internal, generate
  1,  820,    1
*Elset, elset=_PickedSet2, internal, generate
  1,  696,    1
** Section: Filament
*Solid Section, elset=_PickedSet2, material=Filament
1.,
*End Part
**
*Part, name=Nozzle
*Node
   811,   1.24062145,   3.45488214
*Element, type=CAX3T
*Element, type=CAX4T
*Nset, nset=_PickedSet2, internal, generate
  1,  811,    1
```

```
*Elset, elset=_PickedSet2, internal, generate
  1,  704,    1
** Section: Nozzle
*Solid Section, elset=_PickedSet2, material=Steel
1.,
*End Part
**
**
** ASSEMBLY
**
*Assembly, name=Assembly
**
*Instance, name=Nozzle-1, part=Nozzle
*End Instance
**
*Instance, name=Filament-1, part=Filament
        0.,    -0.259777,           0.
*End Instance
**
*Nset, nset=_PickedSet24, internal, instance=Nozzle-1
 24,  25, 170
*Elset, elset=_PickedSet24, internal, instance=Nozzle-1
 146, 240
*Nset, nset=_PickedSet25, internal, instance=Filament-1, generate
  1,  820,    1
*Elset, elset=_PickedSet25, internal, instance=Filament-1, generate
  1,  696,    1
```

*Nset, nset=_PickedSet26, internal, instance=Nozzle-1, generate

1, 811, 1

*Nset, nset=_PickedSet26, internal, instance=Filament-1, generate

1, 820, 1

*Elset, elset=_PickedSet26, internal, instance=Nozzle-1, generate

1, 704, 1

*Elset, elset=_PickedSet26, internal, instance=Filament-1, generate

1, 696, 1

*Elset, elset="_filament contact surf_S4", internal, instance=Filament-1

39, 53, 54, 55, 56, 57, 58, 59, 60, 61, 62, 63, 64, 65, 66, 67

68, 69, 70, 136, 137, 140, 150, 152, 156, 164, 165, 166, 167, 168, 169, 170

171, 172, 174, 175, 176, 177, 178, 179, 180, 181, 182, 183, 184, 185, 186, 187

188, 189, 190, 191, 192, 193, 194, 195, 196, 197, 198, 199, 200, 201, 202, 203

204, 205, 206, 207, 208, 209, 210, 211, 212, 213, 214, 215, 216, 217, 218, 219

295,

*Elset, elset="_filament contact surf_S2", internal, instance=Filament-1

48, 50, 51, 79, 80, 81, 82, 83, 134, 143, 153, 154, 155, 157, 160, 161

162, 163, 220, 221, 289, 290, 302, 316, 330, 436, 675, 677, 678, 679, 687, 689

690, 691

*Elset, elset="_filament contact surf_S3", internal, instance=Filament-1

77, 84, 147, 148, 149, 173, 683

*Elset, elset="_filament contact surf_S1", internal, instance=Filament-1

85, 86, 87, 88, 89, 142, 144, 145, 146

*Surface, type=ELEMENT, name="filament contact surf"

"_filament contact surf_S4", S4

"_filament contact surf_S2", S2

"_filament contact surf_S3", S3

"_filament contact surf_S1", S1

*Elset, elset="_nozzle contact surf_S1", internal, instance=Nozzle-1

23, 24, 25, 26, 27, 152, 153, 154, 233, 269, 270, 271, 272, 275, 278, 279

280, 281, 290, 292, 297, 314, 370

*Elset, elset="_nozzle contact surf_S3", internal, instance=Nozzle-1

157, 161, 273, 274, 282, 283, 284, 285, 286, 287, 288, 289, 295, 321, 684

*Elset, elset="_nozzle contact surf_S4", internal, instance=Nozzle-1

276,

*Surface, type=ELEMENT, name="nozzle contact surf"

"_nozzle contact surf_S1", S1

"_nozzle contact surf_S3", S3

"_nozzle contact surf_S4", S4

*Elset, elset=__PickedSurf22_S3, internal, instance=Filament-1

46,

*Elset, elset=__PickedSurf22_S2, internal, instance=Filament-1

89,

*Surface, type=ELEMENT, name=_PickedSurf22, internal

__PickedSurf22_S3, S3

__PickedSurf22_S2, S2

*Elset, elset=__PickedSurf23_S3, internal, instance=Nozzle-1

16, 47, 51, 67, 76, 90, 99, 103, 104, 146, 235, 634, 662

*Elset, elset=__PickedSurf23_S4, internal, instance=Nozzle-1

17, 35, 145, 238, 646, 663

*Elset, elset=__PickedSurf23_S1, internal, instance=Nozzle-1

19, 42, 58, 94, 231, 234, 236, 237, 641, 664, 665, 666, 668

*Elset, elset=__PickedSurf23_S2, internal, instance=Nozzle-1

106,

```
*Surface, type=ELEMENT, name=_PickedSurf23, internal
__PickedSurf23_S3, S3
__PickedSurf23_S4, S4
__PickedSurf23_S2, S2
__PickedSurf23_S1, S1
*End Assembly
*Amplitude, name="Ramp 2 sec"
          0.,          0.,          2.,          1.
**
** MATERIALS
**
*Material, name=Filament
*Conductivity
 0.21,
*Density
 9.7e-19,
*Elastic, moduli=LONG TERM
1000., 0.4
*Plastic
2.,0.
7.,2.
*Specific Heat
 1e+12,
*Viscoelastic, time=CREEP TEST DATA
*Volumetric Test Data, volinf=1.66
 9.047,62.
*Material, name=Steel
```

*Conductivity

43.,

*Density

7.8e-12,

*Elastic

200000., 0.3

*Specific Heat

5.02e+08,

**

** INTERACTION PROPERTIES

**

*Surface Interaction, name=ContactProp

1.,

*Friction, slip tolerance=0.005

0.2,

*Surface Behavior, pressure-overclosure=HARD

**

** PREDEFINED FIELDS

**

** Name: Predefined Field-1 Type: Temperature

*Initial Conditions, type=TEMPERATURE

_PickedSet26, 100.

**

** INTERACTIONS

**

** Interaction: contact

*Contact Pair, interaction=ContactProp, type=SURFACE TO SURFACE

"filament contact surf", "nozzle contact surf"

** --

**

** STEP: Adiabatic extrude

**

*Step, name="Adiabatic extrude", nlgeom=YES, inc=10000

*Coupled Temperature-displacement, creep=none, deltmx=50., stabilize, factor=0.0002, allsdtol=0, continue=NO

0.001, 10., 1e-06, 0.01

*Solution Technique, type=SEPARATED

**

** BOUNDARY CONDITIONS

**

** Name: nozzle fixation Type: Displacement/Rotation

*Boundary

_PickedSet24, 2, 2

*Adaptive Mesh Controls, name=ALE mesh rule

1., 0.

*Adaptive Mesh, elset=_PickedSet25, controls=ALE mesh rule, op=NEW

**

** LOADS

**

** Name: Heat flux Type: Surface heat flux

*Dsflux

_PickedSurf23, S, 1.

** Name: extrude pressure Type: Pressure

*Dsload, amplitude="Ramp 2 sec"

_PickedSurf22, P, 0.07

**

** OUTPUT REQUESTS

**

*Restart, write, frequency=0

**

** FIELD OUTPUT: F-Output-1

**

*Output, field, variable=PRESELECT

**

** HISTORY OUTPUT: H-Output-1

**

*Output, history, variable=PRESELECT, frequency=5

*End Step*Heading

Vita

Diana Berenice Montes Carrera was born October 12 in 1993 in the small city of Parral, Chihuahua, Mexico. At the age of six, she then moved in the year 2000 to Juarez, Chihuahua and continued her education. In 2004 Diana changed schools to Father Yermo in El Paso, TX where she finished the remaining of her elementary, and high school years. At that time, she realized she had an interest in engineering overall and decided to pursue a degree in Mechanical Engineering. After graduation she started to take some classes at El Paso Community College. Continuing her education, she then transferred to The University of Texas at El Paso. While finishing her degree, she joined MAES/SHPE and volunteered in LIMBS with her interest in prosthetics. After volunteering she started working in different departments of the university as a teaching assistant followed by an internship in Cardinal Health as a process engineer. In December 2016 she graduated with a bachelor's in mechanical engineering. After this she decided to continue her education and pursue a master's degree as well. A spring after graduating she started her post-graduate education in Mechanical Engineering as well. While taking classes, she worked as a teaching assistant throughout her degree. After graduating from UTEP she will then continue grow and expand her skills in the working field to motivate and become an inspiration for future engineers and to others.

Contact Information: dbmontescarrera@miners.utep.edu

This thesis was typed by Diana Berenice Montes Carrera.